The effect of single versus successive warm summers on an intertidal community

Amelia V. Hesketh[1,2*], Cassandra A. Konecny[2], Sandra Emry[2], and Christopher D. G. Harley[2,3]

Author affiliations:

1. School of Resource and Environmental Management, Simon Fraser University, 8405 – TASC 1, 8888 University Dr., Burnaby, BC, V5A 1S6
2. Department of Zoology, University of British Columbia, 4200–6270 University Blvd. Vancouver, BC, V6T 1Z4
3. Institute for the Oceans and Fisheries, University of British Columbia, 2202 Main Mall, Vancouver, BC, V6T 1Z4

* Corresponding author: ahesketh@sfu.ca

Conflict of interest statement:

The authors declare no conflicts of interest.

Ethics statement:

Intertidal organisms were collected under Fisheries and Oceans Canada scientific collection permits (XR 61 2019 and XR 196 2020).

Funding statement:

Funding was provided to A.V. H. through a National Geographic Early Career Grant (EC-54154R-18). Additional support was provided to C. D. G. H. through the Natural Sciences and Engineering Research Council of Canada (NSERC) Canadian Healthy Oceans Network (NETGP 468437-14) and an NSERC Discovery Grant (RGPIN-2016-05441).

Acknowledgements:

This work, from inception to writing, was conducted on the traditional, ancestral, unceded territories of the Coast Salish peoples, including the sovereign Kwikwetlem, Musqueam, Pauquachin, Semiahmoo, Squamish, Tsartlip, Tsawout, Tseycum, and Tsleil-Waututh Nations, whom we thank for their ongoing care for the lands and waters of the Salish Sea. We thank S. Blain, A. Holland, and G. Brownlee for assistance with field work, B. Gillespie and V. Grant for assistance with experimental tile construction, and BC Parks for access to the foreshore at T̓ESNO ̓EN̲ (Ruckle Park). Thanks also to R. Kordas for all the work that came before, and G. Simpson for his exceedingly helpful online resources on additive modeling.

Abstract

To accurately predict how organisms and ecological communities will respond to future conditions caused by climate change, we must consider the temporal dimension of environmental stressors, including the effects of repeated exposures to stress. We performed a two-year passive warming experiment in coastal British Columbia to explore the response of intertidal communities to single and successive warm summers. Elevated summertime temperatures tended to reduce the abundance of barnacles and grazers, algal cover, and alpha diversity compared to ambient temperatures, and both contemporaneous and persistent effects of warming were detected. While elevated summer temperatures appeared to have direct effects on organism survival and growth, the persistent effects of warming through time and differences in community structure between treatments were likely mediated by differences in foundation species (barnacle) abundance between treatments. Unexpectedly, the effects of thermal stress in year two were rarely dependent on whether there had been thermal stress in year one. Our study suggests that, while barnacle beds can recover from single warm summers, recurring thermal stress will result in a more depauperate, less diverse community over time, particularly if foundation species are negatively affected.

Keywords: barnacles, climate change, community, diversity, foundation species, heatwaves, intertidal zone, mortality, warming

Introduction

Warming linked to climate change can have substantial ramifications across ecological scales (Burrows et al. 2020, Bozinovic et al. 2020). In addition to long-term increases in global surface temperatures (IPCC 2023), the frequency and severity of extreme temperature events such as marine and atmospheric heatwaves is expected to increase over the coming decades (Oliver et al. 2018, Perkins-Kirkpatrick and Lewis 2020). Extreme temperatures have biological consequences. Beyond some thermal optimum at which performance peaks, increases in temperature reduce organism performance to the point of death at the thermal maximum (Buckley et al. 2022). Heatwaves increase the probability of environmental temperatures surpassing these thermal thresholds (Vasseur et al. 2014), and thus they can impair fitness (Siegle et al. 2022) and, ultimately, cause mortality (Harley 2008, Hesketh and Harley 2023). If thermally tolerant species survive heatwaves and thermally sensitive species do not, community structure will correspondingly shift, as has been documented in response to marine heatwaves (Weitzman et al. 2021, Montie and Thomsen 2023).

As heatwave frequency is increasing, so, too, are studies of their effects on organisms; however, the consequences of repeated exposures to thermal stress have received less attention. This is particularly true at the community level, where controlled warming manipulations can present an experimental challenge. If environmental stress occurs over a prolonged period, or if repeated stressors occur in rapid succession, there can be stronger negative consequences on organism survival and fitness (Bible et al. 2017; Ma et al. 2018; Siegle et al. 2022). At the community level, repeated stressors that occur with limited intervening time for recovery can produce more homogenous (Hammill and Dart 2022) and depauperate (Dal Bello et al. 2019) communities. Even if recovery can occur between stressors, an initial stressor may engender

93 susceptibility to subsequent stressors (Marshall and Sinclair 2015, Siegle et al. 2018, Jackson et
94 al. 2021, Sun et al. 2022), perhaps by eroding the energy stores available for coping with
95 secondary stressors. Alternatively, if an initial stressor increases performance or induces the
96 production of protective metabolites, organisms may instead be more robust to subsequent
97 stressors (Marshall and Sinclair 2015, Brooks and Crowe 2019, MacLennan and Vinebrooke
98 2021, Agrawal and Jurgens 2023). Manipulating the timing of stressors, in addition to their
99 intensity, is key to better understanding their ecological effects.
100 Though temperature greatly influences organisms, the reverse is also true. Foundation
101 species (Dayton 1971) create complex biogenic habitat, which can provide thermally benign
102 microhabitats for associated organisms, primarily through shading and moisture retention
103 (Hesketh et al. 2021, Lee et al. 2021, Jurgens et al. 2022, Christiansen et al. 2022, Gutiérrez et
104 al. 2023). While the loss of foundation species often negatively impacts associated species
105 (Ellison 2019), habitat formers may act as important facilitators even in death, leaving behind
106 structures that can bolster recruitment (Liversage et al., 2020) and provide thermal refugia for
107 motile organisms (Uyà et al. 2020, Hesketh and Harley 2023). The importance of such
108 facultative facilitations for bolstering organism survival and performance may increase with
109 environmental stress, though there may be an upper limit beyond which stress cannot be
110 effectively buffered (Bruno et al. 2003, He et al. 2013, Bulleri et al. 2016).
111 Within the intertidal zone, where many species live at or near their upper thermal limit
112 (Tomanek and Helmuth 2002, Harley 2011), barnacles are commonly occurring organisms that
113 facilitate a relatively diverse community via the provision of biogenic habitat (Harley 2006,
114 Hesketh et al. 2021). Barnacles can provide an attachment surface and grazing refuge for algae
115 (Farrell 1991, Geller 1991), as well as retain moisture (Vermeij 1978, Harley and O'Riley 2011)

and provide shade (Cartwright and Williams 2014), thereby reducing the substratum temperature for closely associated species. Even empty barnacle tests serve as humid, thermally benign microhabitats for a diverse community (Reimer 1976, Barnes 2000, Chim et al. 2016). While historically considered robust, the resilience of rocky intertidal communities is beginning to erode due to repeated thermal disturbance, among other stressors (Menge et al. 2022). Declines in barnacle abundance and increases in barnacle mortality have been attributed to increases in temperature (Little et al. 2021) and heatwaves (Hesketh and Harley 2023), which can also impact the diversity, composition, and organism abundance in barnacle-associated communities (Kordas et al. 2015, Hesketh and Harley 2023).

In this study, we tested the effect of single and successive warm summers on high intertidal barnacle bed communities dominated by *Balanus glandula* (Darwin 1854) through a two-year passive warming experiment. Substratum temperatures were manipulated by deploying black (warm) and white (cool) settlement tiles in the intertidal zone following an established method (Kordas et al. 2015). After one year, the treatments of half of the experimental tiles were swapped to manipulate the temporal dimension of thermal stress. We hypothesized that, because warming may reduce organism performance and increase mortality, communities exposed to warm temperatures, even for a single year, would have lower invertebrate abundance, algal cover, and diversity than those that experienced cool conditions. Further, we hypothesized that the effects of thermal stress in year two would be stronger in communities that were previously exposed to thermal stress due to pre-existing reductions in foundation species cover, and thus reduced availability of thermal refugia.

Materials and methods

Site description

This study was completed near T̓ESNO꞉EN̲ (Beaver Point), a site in the Salish Sea that lies within the traditional, unceded territory of the W̱SÁNEĆ peoples in what is now known as Ruckle Provincial Park on Salt Spring Island, British Columbia (48.77324, -123.36637). The substratum at this site is dominated by a southeast-facing semi-exposed sandstone bench, and tides are mixed semi-diurnal. Relative to the rest of British Columbia's southern Gulf Islands, this area is exposed to cooler, more saline water and larger waves due to its proximity to Haro Strait and the Strait of Juan de Fuca. This site also receives regular commercial ferry wake, with potential implications for intertidal community composition (Demes et al. 2012). However, like the rest of the Canadian southern Gulf Islands and neighboring San Juan Islands (USA), the intertidal zone at this site is considered a thermal "hot spot" due to its summertime midday low tides coupled with relatively clear, sunny weather (Helmuth et al. 2006) that make it particularly susceptible to atmospheric heatwaves (e.g., Raymond et al. 2022).

The upper intertidal zone at this site is dominated by the acorn barnacles *Balanus glandula* and *Chthamalus dalli*, with sporadic beds of the perennial brown alga *Fucus distichus* and patches of the crustose *Petrocelis* phase of *Mastocarpus* sp.. Filamentous ephemeral algae occur as early colonizers of bare space (predominantly the green algae *Ulothrix* sp. and *Urospora* sp.) and foliose ephemeral algae occur in winter, often attached to underlying barnacles (predominantly *Ulva* spp., *Pyropia* sp., and *Petalonia fascia*). Herbivore species include the littorine snails *Littorina scutulata* and *L. sitkana* and the limpets *Lottia paradigitalis, L. digitalis*, *L. pelta*, and *L. scutum*. Herbivores are relatively plentiful throughout the intertidal zone, though thermally sensitive species migrate down shore with the onset of daytime low tides

and warmer temperatures in spring and return to higher tidal elevations in August (Kordas et al. 2015).

Study design

Individual settlement tiles were built based on previous methods (Kordas et al., 2015; see Appendix 1 for further fabrication details). In brief, each 15x15 cm tile consisted of a central epoxy settlement surface bordered by either white (cool treatment) or black (warm treatment) high-density polyethylene (6.4 mm thick; Redwood Plastics, Vancouver, Canada). Temperature differences were driven by differences in the absorption of incoming solar radiation during daytime summer low tides. Settlement areas were 6.9×6.9 cm and composed of a thin layer (< 5 mm) of Sea Goin' Poxy Putty (Permalite Plastics, Rancho Dominguez, CA, USA). These settlement tiles were affixed to a bottom tile unit composed of thicker white high-density polyethylene (9.5 mm thick; Redwood Plastics, Vancouver, Canada) that was used to anchor the assembly to the underlying bedrock (Appendix 1 Fig. A2a). An iButton temperature logger (model DS1921G-F5# Thermochron, Dallas Semiconductor) was sandwiched between the two units just under the surface of the epoxy settlement surface to measure substratum temperature.

This study followed a randomized block design, with six experimental blocks consisting of 16 tiles each, eight of which were black and eight of which were white (N=96). Tiles were installed on 12 April 2019 at a shore level of 2.34 ± 0.07 m above Canadian chart datum. On 3 April 2020, we randomly chose half of the black and half of the white tiles in each block and swapped the colour of these tiles with white and black heavy-duty tape (Gorilla Tape, Gorilla Glue, Inc., Cincinnati, OH, USA; adhesion enhanced with LePage Ultra Gel super glue), while the remainder were left unaltered (Fig. A2b). This change resulted in four thermal history

185 treatments during the second year of the study (cool summer–cool summer, CC; cool–warm,
186 CW; warm–cool, WC; and warm–warm, WW). The study was originally designed with n=24
187 tiles per treatment, four in each of six blocks; however, there was some variation in sample size
188 through time as tiles were lost due to dislodgement or log damage (Appendix 1: Fig. A3). Early
189 attempts to simultaneously manipulate herbivore populations were unsuccessful due to wave and
190 temperature regimes at the site (see Appendix 1), but these initial manipulations did not
191 significantly influence community responses.
192
193 *Temperature measurement*
194 Substratum temperature of both settlement surfaces and adjacent bedrock were collected
195 using pre-programmed iButton temperature loggers (model DS1921G-F5# Thermochron, Dallas
196 Semiconductor). iButtons recording tile surface temperatures were sealed in nitrile pouches and
197 sandwiched between the two plates of each experimental tile unit (Fig. A1). One logger per
198 block was used to record bedrock substratum temperature. These loggers were wrapped in
199 Parafilm and affixed to shore with a 2–3 mm layer of A–788 Splash Zone epoxy (Pettit Paints,
200 Rockaway, NJ, USA) separating the logger from both the underlying shore and surrounding air.
201 The number of loggers recording data varied through time for each treatment as the number of
202 treatment groups changed between years and due to instrument failure. In the first and second
203 years, between 3–8 and 1–4 temperature loggers, respectively, were present in each treatment
204 within each block. At least four temperature loggers were always simultaneously recording
205 bedrock temperature across blocks (excepting 18 July–19 August 2020, for which no data exist).
206 Temperatures were recorded hourly except over the second winter of the study, when
207 temperatures were instead recorded every two hours.

208

209 *Community surveys*

210 We recorded organism abundance and cover at monthly intervals during summer and
211 every two months during winter from 12 April 2019 to 24 February 2021, when the last of the
212 tiles were removed. During these surveys, each organism was identified to the species level
213 except for amphipods and isopods, which were identified to order. Invertebrates were counted,
214 while the percent cover of each alga was recorded with the aid of a small wire quadrat. Sessile
215 species were only recorded within the central 6×6 cm area of the epoxy settlement surface to
216 avoid edge effects. Motile invertebrates were counted on the entire tile surface since their
217 influence on the experimental community could not be ruled out.

218 To measure total epifaunal diversity on each tile immediately after high summer
219 temperatures and after a winter recovery period, we destructively sampled half of the tiles in
220 each treatment group within each experimental block on 14 September 2020 and the remainder
221 on 24 February 2021. During sampling, all barnacles and associated fauna were scraped from the
222 tile's surface into specimen containers and preserved in 70% ethanol (v/v in water). Epifauna
223 were later identified and counted under a dissecting microscope.

224

225 *Statistical analyses*

226 All analyses were performed in R version 4.3.2 (R core team 2023). We used linear
227 mixed effects models, constructed with *lme4* (version 1.3-33, Bates et al. 2015), to test for
228 thermal differences between experimental treatments. Because temperatures within treatments
229 were driven by solar irradiance, temperature data were retained only if they were collected (1)
230 when the tile was emersed at the time of recording (for details on estimating tile shore level, see

231 Appendix 1), (2) after sunrise and before sunset, and (3) between 15 June and 31 August, when
232 treatment differences were expected to be strongest. These temperature data were used to
233 calculate the mean and mean daily maximum daytime temperatures of individual tiles, which
234 were modeled, along with the absolute maximum summertime temperature, as a function of
235 treatment. Mean daily maxima are a particularly good measure of thermal stress for ectotherms
236 such as barnacles that have low profiles and relatively large areas of attachment to the
237 substratum (LaScala-Gruenewald and Denny 2020). A random effect of date and of tile number
238 nested within experimental block were included to account for repeated measures and spatial
239 effects.

240 We then used generalized linear mixed models, created with *glmmTMB* (version 1.1.7;
241 Brooks et al. 2017), to determine how temperature treatment affected the abundance of key taxa
242 and alpha diversity at the end of summer and at the end of winter. During the first year, barnacle
243 recruitment and abundance, grazer abundance, and alpha diversity were modeled as a function of
244 the treatment (cool or warm), while during the second year, these data were modeled as a
245 function of the interaction of treatments applied in year one and year two. When multiple dates
246 were modeled within a single year, date was also included as a fixed effect. Because no *a priori*
247 hypotheses were made about this term, date was included as either an interactive or additive
248 effect, whichever generated the most parsimonious model (determined by comparing model
249 AIC). Experimental block was included as a random effect. A fixed effect for herbivore
250 manipulations attempted early on in the study was not included, since this did not substantially
251 improve the fit of any model ($\Delta AIC < 2$). Model fit was evaluated using the *DHARMa* package
252 (version 0.4.6; Hartig 2022) and models were analyzed by ANOVA through the *car* package
253 (version 3.1-2; Fox and Weisberg 2019) with a significance threshold of $p = 0.05$, either a Type

III or Type II sum of squares if an interaction term was or was not hypothesized, respectively. The *emmeans* package (version 1.8.6; Lenth 2022) was used for Tukey-Kramer *post hoc* pairwise comparisons of treatment groups.

We used generalized additive modeling with the *mgcv* package (version 1.9.0; Wood 2011) to analyze how the temperature treatments shaped algal cover during each year of the study. Within these models, we included a parametric effect of thermal treatment, a random effect of block, and — to examine temporal trends between treatments — separate smoothed functions of time for each treatment. Pairwise differences in algal cover over time between control treatments (C and CC) and other treatments were calculated and visualized using established methods (Rose et al. 2012).

Treatment-driven differences in epifaunal community structure and beta diversity were modeled using the *vegan* package (version 2.6-4; Oksanen et al. 2020). Data were ordinated using distance-based redundancy analysis (function *dbRDA*) with Bray-Curtis distances. PERMANOVA analyses were performed with 9999 permutations constrained within experimental blocks using the *anova.cca* function. Multiple pairwise comparisons were made with *multiconstrained* in the *BiodiversityR* package (2-15.4, Kindt and Coe 2005). PERMDISP analyses were run with bias adjustment for small sample sizes.

Results

Substratum temperature

Mean daily maximum substratum temperatures were significantly greater in passively warmed treatments compared to cool treatments in both the first summer (Figure 1; ANOVA: $F_{2,72} = 15.04$, $p < 0.001$) and the second summer (ANOVA: $F_{4,66} = 10.49$, $p < 0.001$) of the study. During the first year, the cool and warm treatments had average summertime daily maximum temperatures of 28.3 ± 6.5 ºC and 30.4 ± 7.7 ºC (mean ± SD), respectively. Bedrock temperatures were 30.3 ± 6.5 ºC, which were statistically similar to those of the warm treatment and significantly higher than temperatures in the cool treatment (Tukey-Kramer: z ratio = -5.29, $p < 0.001$). Similar patterns of daily maximum temperature were recorded in the second year (28.3 ± 5.7 ºC and 28.4 ± 5.8 ºC in WC and CC treatments versus 30.5 ± 6.7 ºC and 30.7 ± 6.3 ºC in WW and CW treatments, respectively), but bedrock temperatures (27.4 ± 5.9 ºC) were statistically similar to those of all other treatments (Tukey-Kramer: $p > 0.05$). Treatments where tape was present on tile surfaces (WC and CW) had similar temperatures to analogous treatments where tape was absent (CC and WW, respectively; Appendix 2, Table A6). Trends in mean and absolute maximum temperatures were similar to trends in average daily maximum temperature (Appendix 1: Fig. A5, Tables A7–14).

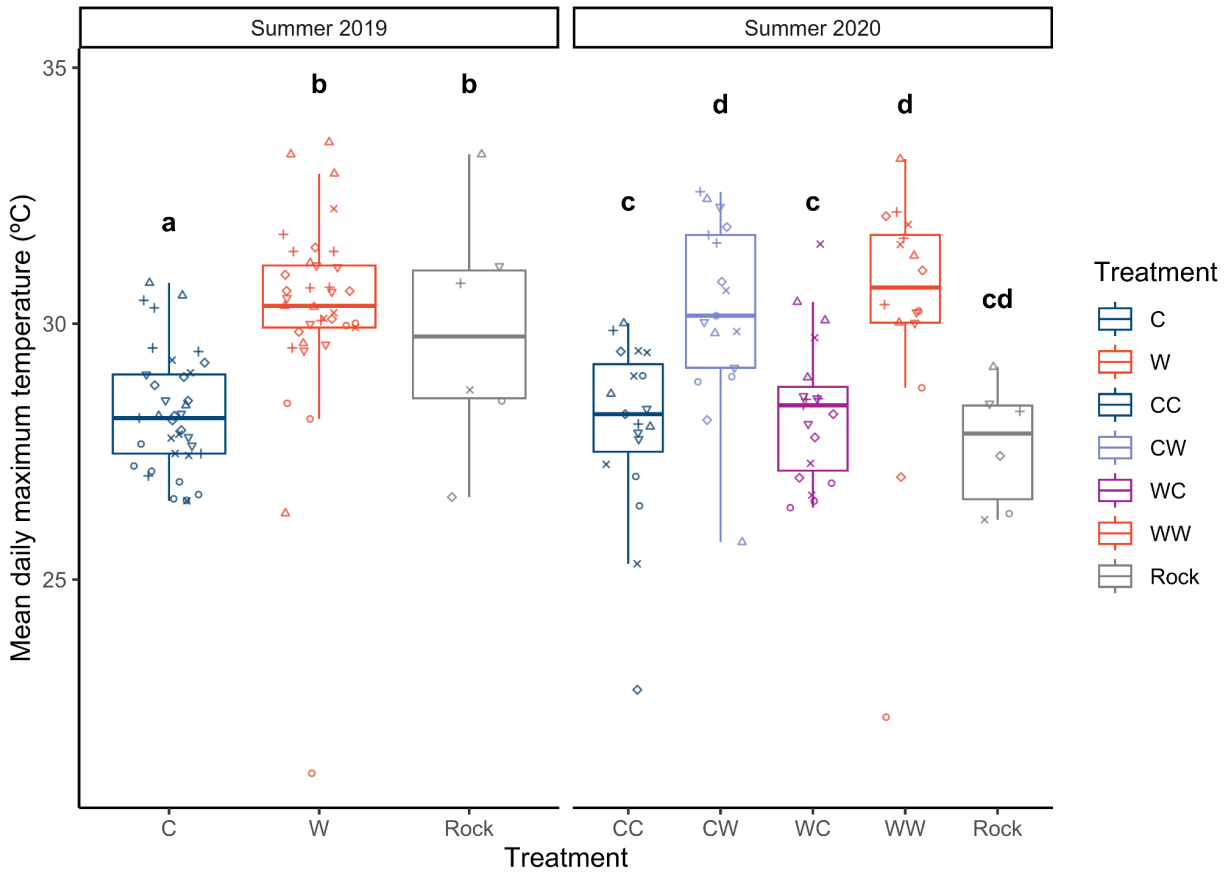

296

297 **Figure 1.** Differences in mean daily maximum substratum temperatures of experimental tiles and
298 adjacent bedrock recorded by embedded temperature loggers at TESNO, EN, Salt Spring Island.
299 Points represent the mean value for each experimental tile for which temperature was measured,
300 with different shapes used to represent each experiment block. Only temperature data collected
301 during daytime summer low tides between 15 June – 31 August were used. Due to sporadic
302 logger failures, the temperatures of tiles were not necessarily recorded for the entire period, and
303 the number of temperature loggers within each treatment varied over time. Bold lowercase letters
304 represent statistically different groups, as determined by Tukey-Kramer *post hoc* tests on
305 temperature models. C = cool summer, W = warm summer, CC = cool–cool, CW = cool–warm,
306 WC = warm–cool, WW = warm–warm.

Changes in barnacle abundance

The abundance of the acorn barnacles *B. glandula* and *C. dalli* varied substantially through time due to natural patterns of spring recruitment and post-recruitment summer mortality (Appendix 2: Fig. A6). In general, warm summer temperatures tended to cumulatively reduce the abundance of barnacle recruits and adults. When recruitment was at its maximum during the first year of study (May and June, respectively, for *B. glandula* and *C. dalli*), temperature treatment did not affect *B. glandula* recruitment (Fig. 2a; Appendix 2: Table A15), but *C. dalli* recruitment was greater in the cool treatment relative to the warm treatment (Fig. 2b; Type II ANOVA, χ^2_1= 4.13, p = 0.0422). However, at the end of the first year, there were substantially more adult *B. glandula* in the cool compared to the warm treatment (Fig. 2c; Type II ANOVA; χ^2_1=106.20, p < 0.001), while *C. dalli* abundance was similar between treatments (Appendix 2: Table A24). During peak recruitment in the second year of study, warm temperatures suppressed *B. glandula* recruitment, whether warming was applied contemporaneously (Type III ANOVA, treatment_{y2}; χ^2_1=38.34, p < 0.001) or during the previous summer (treatment_{y1}; χ^2_1=6.07, p = 0.0138). *Chthamalus dalli* recruitment was also reduced by warm temperatures, whether warming occurred during the second (Fig. 2d; Type III ANOVA; χ^2_1=19.16, p < 0.001) or the first summer (χ^2_1=5.56, p = 0.0184). At the end of the study, final barnacle abundance was not significantly related to temperature manipulation in either year (Appendix 2: Tables A22, A25). However, *B. glandula* abundance appeared to be negatively related to warming in both summers (though trends were non-significant; p ~ 0.1; Appendix 2: Table A22), and *post hoc* testing suggested that *B. glandula* abundance was greater in the consistently cool treatment (CC) compared to the consistently warm treatment (WW; Tukey-Kramer; z ratio = 3.08, p = 0.0111).

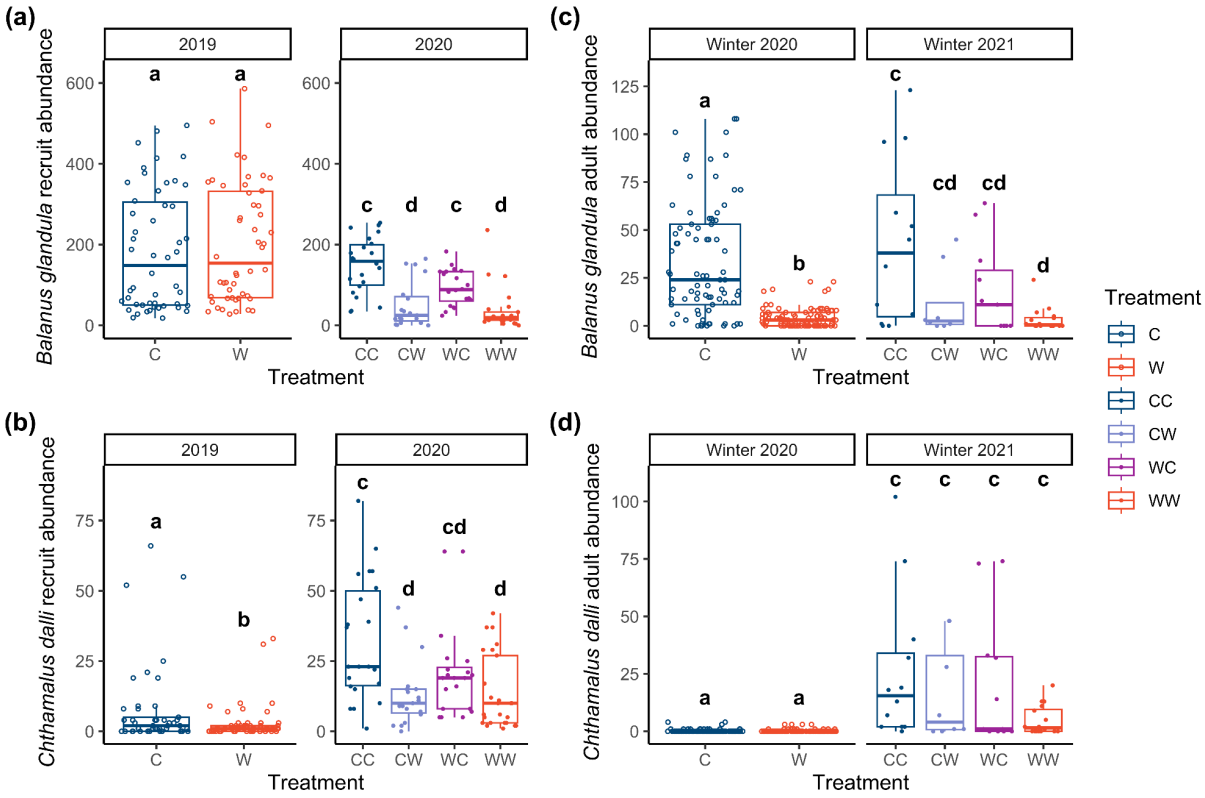

Figure 2. Treatment-driven differences in acorn barnacle abundance during a two-year passive warming manipulation at TESNO, EN, Salt Spring Island, in terms of **(a)** abundance of *B. glandula* recruits (9 May 2019: n = 50; 4 June 2020: n = 22, 19, 20, 25 for CC, CW, WC, and WW) and **(b)** *C. dalli* recruits during peak recruitment (5 June 2019: n = 46, 50 for C and W, respectively; 4 June 2020: n = 22, 19, 20, 25 for CC, CW, WC, and WW) and **(c)** abundance of adult *B. glandula* and **(d)** adult *C. dalli* on experimental tiles at the end of the first and second winters (Winter 2020: n=82 for C, n=91 for W; Winter 2021: n = 12, 8, 11, 16 for CC, CW, WC, and WW). Peak recruitment was recorded on 9 May 2019 and 5 June 2019 in Year 1 for *B. glandula* and *C. dalli*, respectively, and occurred for both species on 4 June 2020 in Year 2. Letters indicate significant differences between treatment groups determined by Type II

ANOVA (year one) or from Tukey-Kramer *post hoc* tests (year two). Treatment codes as in Fig. 1.

Changes in grazer abundance

Differences in grazer abundance between treatments were tested only during the second year of study because grazer communities were constrained during the first summer of the study (see Appendix 1). Warm temperatures, whether experienced during the first or second summer of study, correlated with lower grazer abundances. Across both survey dates, warm temperatures exerted a negative contemporaneous effect on grazer abundance (Fig. 3; Type III ANOVA; $\chi^2_1=7.75$, $p < 0.001$ and $\chi^2_1=18.97$, $p < 0.001$ for limpets and littorines, respectively). In addition, warming applied during the first summer (WC and WW treatments) had a persistent negative effect on grazer abundance (Type III ANOVA; $\chi^2=4.10$, $p = 0.0428$ and $\chi^2=22.82$, $p < 0.001$ for limpets and littorines, respectively). Grazer abundances also changed over time during the second year; limpet abundance significantly increased between the end of summer and the winter (Type III ANOVA; $\chi^2_1=19.21$, $p < 0.001$), but the reverse was true for littorine snails (Type III ANOVA; $\chi^2_1=49.65$, $p < 0.001$).

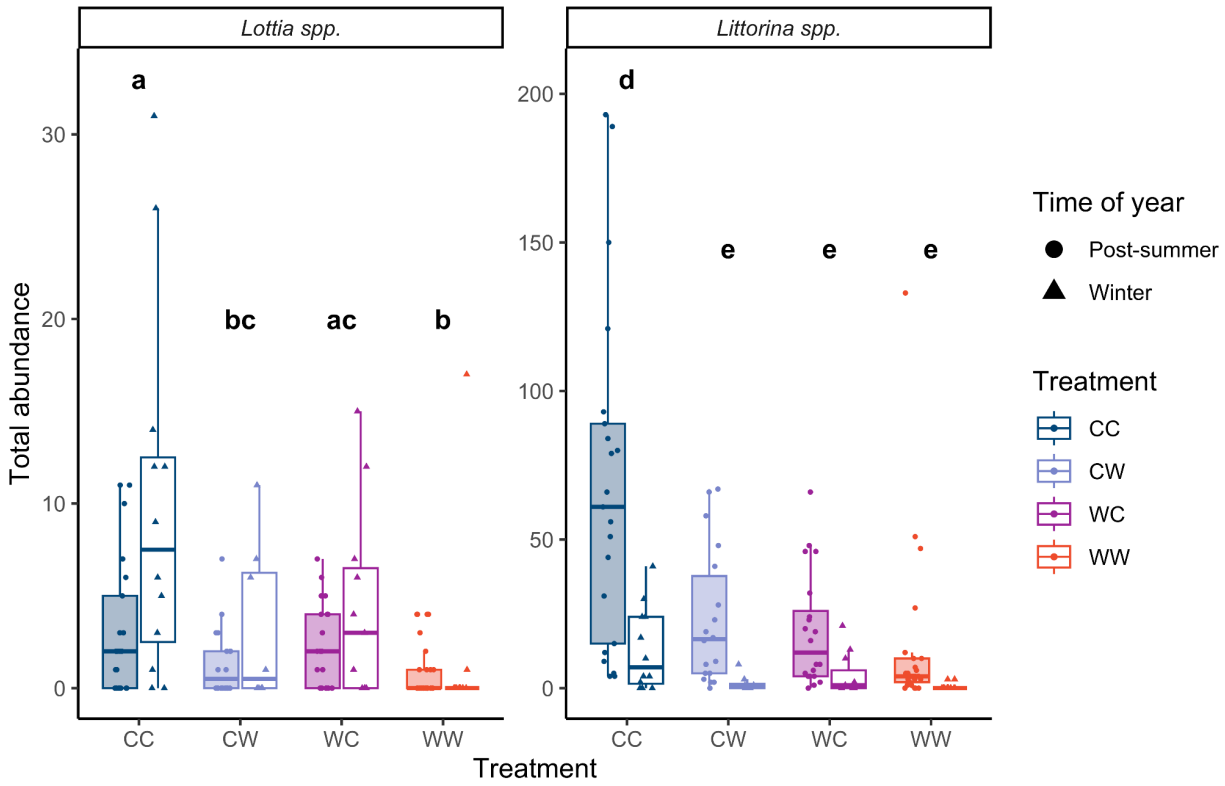

Figure 3. Abundance of *Lottia* spp. (limpets) and *Littorina* spp. (littorine snail) grazers on experimental tiles subjected to different temperature treatments at TESNO, EN, Salt Spring Island immediately following summer (shaded boxes; September 2020; n = 21, 18, 20, 25 for CC, CW, WC, and WW) and during winter (unshaded boxes; February 2021; n = 12, 8, 11, 16 for CC, CW, WC, and WW). Grazers were counted on the entire 15 x 15 cm upper surface of the tiles. Note different y-axis scales for each taxon. Bold lowercase letters indicate significant differences between treatment groups determined by Tukey-Kramer *post hoc* tests. See Fig. 1 for treatment codes.

Changes in algal cover

Algal cover demonstrated substantial non-linearity through time, with differences in the timing of algal blooms and declines between treatments (Fig. 4a). During the first year, algal cover reached its maximum near the end of the summer, driven by a bloom of the green ephemeral alga *Ulothrix* sp., after which cover rapidly declined. While algal cover on tiles was similar between treatments, cover peaked earlier and declined more rapidly within the cool treatment relative to the warm treatment. This resulted in algal cover being initially lower within the warm treatment, but remaining significantly higher until the onset of the first winter (Fig. 4b; *gamm*; $F_6 = 12.61$, $p < 0.001$). Throughout the second year of study, algal cover remained low. While cover was again similar between treatments, the warm–cool treatment had significantly greater cover than the consistently cool (control) treatment by the end of the experiment (*gamm*; $F_2 = 7.47$, $p = 0.00593$).

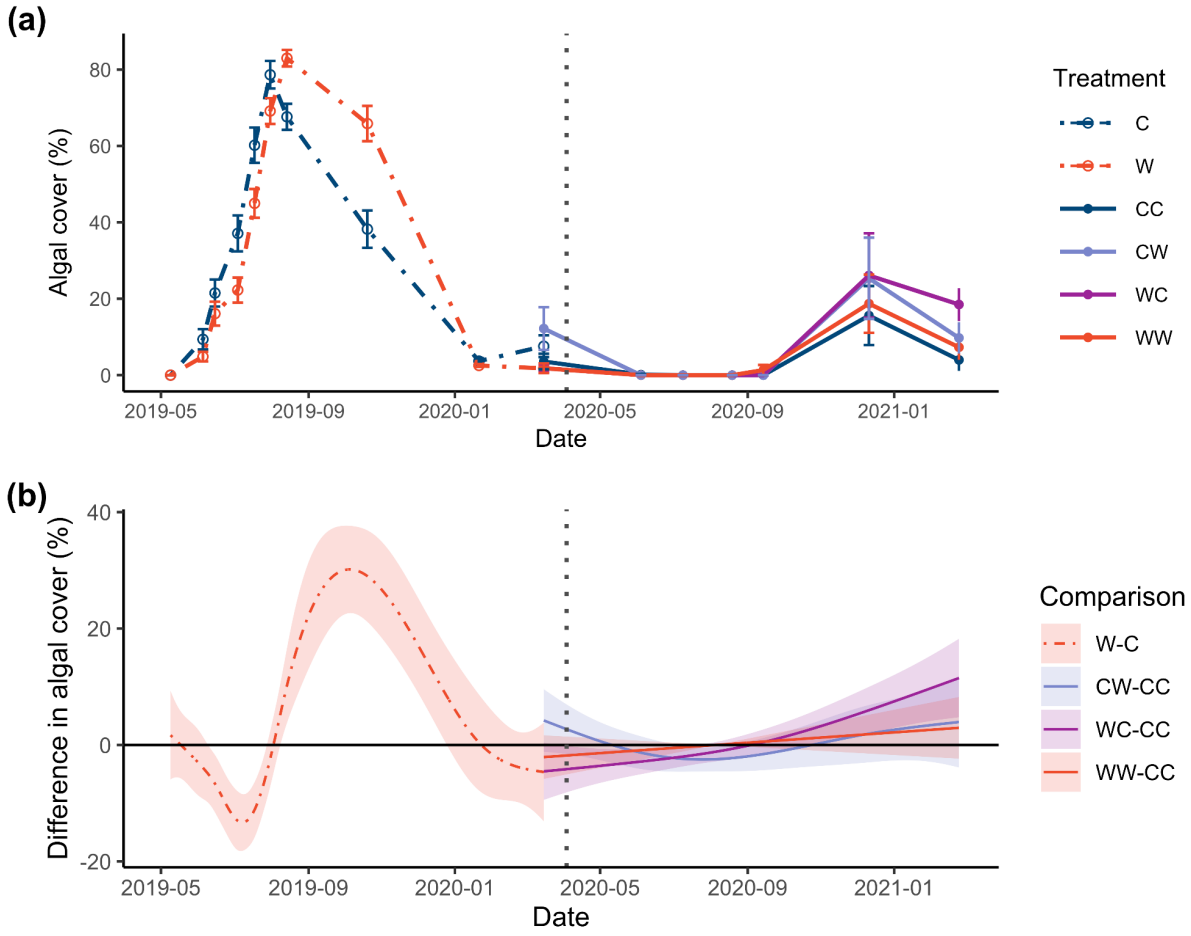

381

382 **Figure 4. (a)** Percent cover of algae on experimental tiles subjected to different summertime
383 temperatures at TESNO, EN, Salt Spring Island over the entire study period. **(b)** Differences
384 between fitted smooth functions of algal cover over time between the control (C or CC)
385 treatment and all other treatments. The shaded area about each line represents an approximate
386 95% pointwise confidence interval; when this area does not overlap the zero line, a significant
387 difference from control conditions can be inferred. The vertical dotted line represents the date at
388 which treatment conditions were changed between year one and year two of the study.

389

390

Changes in diversity

Species richness peaked in winter during both years of the study, typically declining to its lowest point with the onset of daytime lower low tides in spring (Appendix 1: Fig. A8a). Warming tended to reduce alpha diversity and alter community structure, particularly in communities that experienced successive warm summers. During the first year, warm summertime temperatures reduced species richness within communities, and this negative effect was more pronounced in winter than it was immediately following the summer (Fig. 5a; *glmm*, Type III ANOVA; χ^2=9.851, p = 0.00170). During the second year, treatment was not found to have a significant effect on species richness by ANOVA (Fig. 5b; Appendix 2: Table A33). However, *post hoc* pairwise comparisons showed a significant difference between those treatments that were cool during the second summer and the treatment that was successively warmed (Tukey-Kramer; CC–WW: z ratio = 4.16, p < 0.0001; WC–WW: z ratio = 3.28, p = 0.00570). Warming exerted a similar negative effect on the Shannon diversity of the invertebrate community; during winter of the first year, Shannon diversity was significantly lower within the warm treatment, and during the second year, Shannon diversity was lower in treatments where warming was applied during the first year (Appendix 1: Fig. A9a-b, Appendix 2: Tables A35–37). The Shannon diversity of the algal community, meanwhile, was reduced by warm temperatures during the first year, but not during the second year (Appendix 1: Fig. A9c, Appendix 2: Tables A38–40).

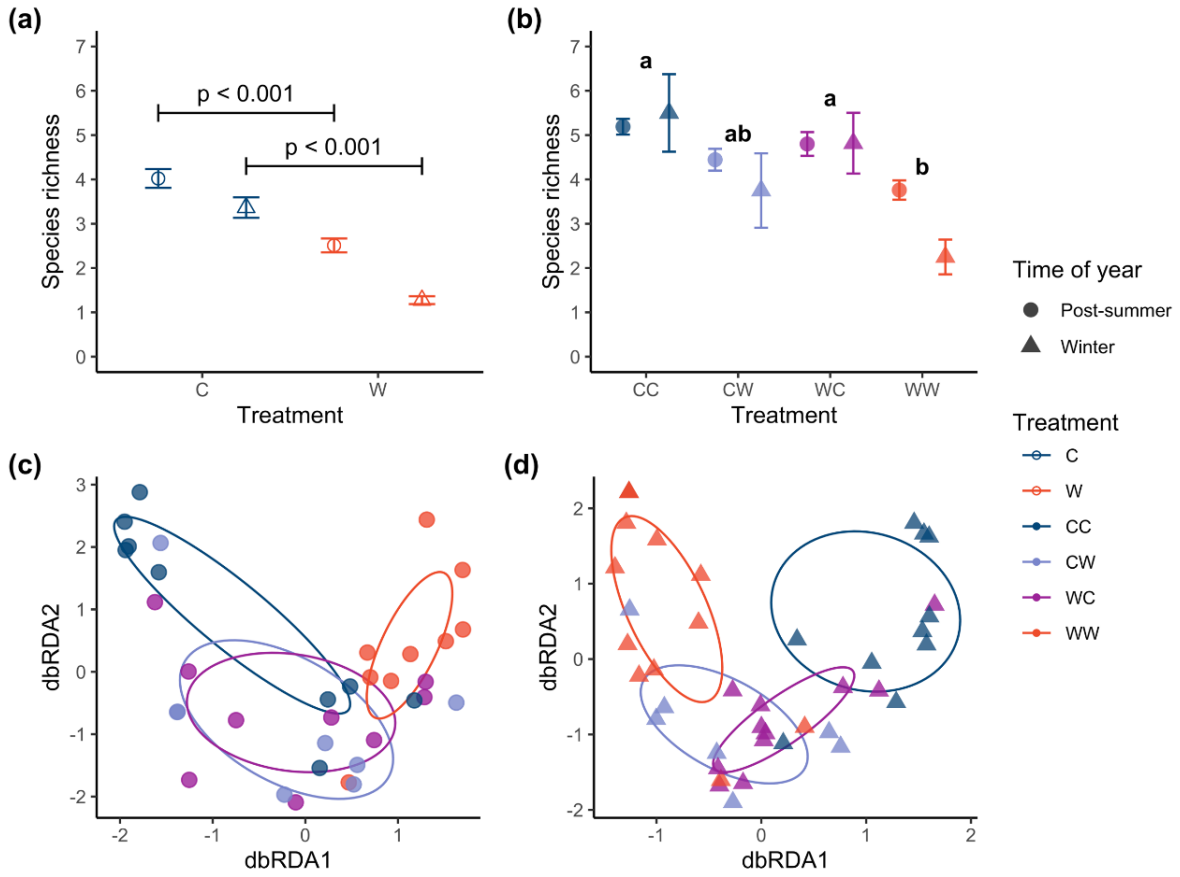

410

411 **Figure 5.** The diversity of intertidal barnacle bed communities subjected to different substratum
412 temperature treatments during a multi-year passive warming manipulation at TESNO, EN, Salt
413 Spring Island. **(a)** Species richness in year one and **(b)** in year two of the experiment, determined
414 from visual surveys after summer and during late winter. Error bars represent standard error
415 about the mean. Differences between treatment groups determined by pairwise comparisons are
416 indicated visually using either asterices (year one) or letters (year two). **(c)** Differences in
417 epifaunal community structure collected by destructive sampling immediately following the
418 second summer (September 2020) and **(d)** at the end of the experiment (February 2021).
419 Community structure plots show data in multidimensional space following ordination using
420 distance-based redundancy analysis using Bray-Curtis distances, with each point representing a

single experimental tile. In Year 1, n = 47 and 49 for C and W, respectively post-summer and n = 41 and 46 for C and W, respectively in winter. For Year 2, n = 21, 18, 20, 25 for CC, CW, WC, and WW post-summer and n = 12, 8, 11, 16 for CC, CW, WC, and WW during winter.

Epifaunal communities isolated from destructively sampled tiles demonstrated that community structure, but not beta diversity, differed between treatments. Following the end of the second summer (September 2020; Fig. 5c), differences in community structure were marginally insignificant (PERMANOVA; $F_{3,31}$=1.495, R^2=0.1264, p = 0.0542), though pairwise comparisons indicated the CC and WW treatments differed in composition (*multiconstrained*; F_1=2.705, p = 0.028). By the end of the experiment (February 2021; Fig. 5d), however, communities diverged significantly in their composition among treatments (PERMANOVA; $F_{3,37}$=3.341, R^2=0.2132, p < 0.001). Pairwise comparisons showed that this was primarily driven by differences between the consistently cool treatment and all others, and from differences between the WC and WW treatments (Appendix 2: Table A44). Beta diversity among communities was similar across treatments (Appendix 2: Table A45–A46). Trends in the alpha diversity of these destructively sampled epifaunal communities were similar to those observed from visual surveys alone (Appendix 1: Figure A10; Appendix 2: Tables A47–50).

Discussion

During this study, we passively manipulated the substratum temperature of intertidal settlement tiles over two years to determine 1) the effect of warmer temperatures on organism abundance and community diversity and 2) whether thermal history from the prior year influences the impact of thermal stress in the subsequent year. We expected that the abundance of key taxa (e.g., barnacles, grazers, algae) and community diversity would be greater under cool conditions where lethal high temperatures were less likely to occur. Because of this, we anticipated that warming during the second summer would exert a weaker effect where temperatures had previously been cool. That is, we expected that cool conditions during the first summer would increase foundation species cover, resulting in more thermally benign microhabitats, which would allow more associated organisms to survive when they experienced subsequent warming. As anticipated, we found that warming generally exerted a negative contemporaneous effect on invertebrate abundance and the alpha diversity of communities, though its effects on algae were more complex. Unexpectedly, the effects of warming in the second summer were independent of whether warming had been applied in the first summer. However, warming applied in the first year frequently had persistent negative effects a year or more later.

The methodology used to manipulate temperature in this study was effective in increasing both the maximum and mean substratum temperatures of experimental communities. In both years, the surfaces of white tiles were cooler than those of black tiles, as in previous manipulations using this system (Kordas et al. 2015, 2017). Interestingly, bedrock temperatures were more analogous to those of black tiles during the first year and white tiles during the second year. This unexpected pattern could be an artefact of shading from copper fences, which encircled tiles for most of the first summer, but not the second. Despite this, temperature

differences between white (cool) and black (warm) tiles were significant, and these drove clear biological differences between treatments.

Acorn barnacles (*B. glandula* and *C. dalli*) recruited onto tiles during spring and early summer each year, and abundance was typically lower within warm treatments for both species, as in past studies (Kordas et al. 2015, 2017, Kordas and Harley 2016). While elevated temperatures can directly affect barnacle abundance and recruitment by reducing performance and survival, the tendency of barnacles to settle gregariously may magnify these negative effects if warming is sustained. The most abundant barnacle observed, *B. glandula*, has a measured LT_{50} in air between 40.5 ºC (Gilman et al. 2015) and 43 ºC (Hamilton and Gosselin 2020), though the onset of mortality has been observed at 40 ºC (Gilman and Rognstad 2018, Ober et al. 2019). Substratum temperatures for tiles within all treatments exceeded these thresholds during daytime summer low tides, and temperatures of 45 ºC were reached in warm treatments during both years, which may explain lower recruit and adult survival therein. Even exposure to temperatures below critical thermal limits can incur metabolic costs. For instance, elevated, non-lethal temperatures can impair the respiration of *B. glandula* many hours after stress exposure (Ober et al. 2019), and sustained warm temperatures can slow barnacle growth (Kordas and Harley 2016). Barnacles preferentially recruit to areas containing conspecifics, a strategy that increases the likelihood of successful sexual reproduction via internal fertilization (Wu 1981). This tendency of barnacles may have generated the observed persistent effect of warming on barnacle abundance across years; tiles that were warmed during the first summer hosted fewer adult barnacles, which then resulted in reduced recruitment during the subsequent year. *Chthamalus dalli*, another acorn barnacle at this site, was not prevalent during the first year, possibly due to interannual variation in recruitment dynamics common in barnacles (Scrosati and Ellrich 2016).

490 Recruitment in the second year was lower within warm treatments, but adult survival was
491 unaffected by temperature treatment, possibly because this species is more robust to thermal
492 stress, with an LT_{50} of 44.5 ºC (Hamilton and Gosselin 2020).
493 Reduced grazer abundance in the warm treatments may have been due to the direct
494 effects of temperature and/or indirect effects mediated by differences in barnacle abundance.
495 One limpet that was commonly observed, *Lottia digitalis*, has an upper thermal limit of 38 ºC in
496 air (Bjelde and Todgham 2013). High intertidal littorine snails have slightly greater tolerance to
497 elevated temperatures (41.01 ºC for *L. sitkana* and 41.47 ºC for *L. scutulata* during five-hour
498 emersions; Stickle et al. 2017). While these dominant grazers are thermally robust, recorded
499 summer temperatures frequently exceeded these thresholds for short periods, and temperatures
500 likely regularly fluctuated above grazer thermal optima (e.g., 30 ºC for *L. digitalis*; Bjelde and
501 Todgham 2013). These sublethal temperatures can have consequences such as suppressed grazer
502 activity, and thus foraging effectiveness (Rickards and Boulding 2015). Only once high
503 temperatures subsided at the end of the summer did we observe gastropod grazers migrating onto
504 tiles. Grazer activity may have been underestimated during surveys at low tide since certain
505 intertidal grazers are only active when the substratum is submerged or awash with the tide (Little
506 1989). However, these temporal dynamics of grazer presence and absence suggest that, while
507 temperature may have directly affected grazer abundance, warming more likely affected these
508 organisms indirectly. Limpets and littorine snails were generally more abundant within cool
509 treatments where barnacle cover was higher, as has been observed in other studies (Creese 1982,
510 Qian and Liu 1990, Silva et al. 2015, Hesketh et al. 2021). When temperatures are high,
511 barnacles may directly benefit associated organisms by creating thermally benign microhabitats
512 through moisture retention (Harley and O'Riley 2011) and/or shading (Cartwright and Williams

2014), thereby reducing mortality and stress (Garrity 1984). During winter, when grazers were most abundant in this study, barnacles may have instead provided refuge from cold stress (Reid and Harley 2021) and hydrodynamic force (Barnes 2000).

Barnacles, in addition to providing microhabitats, may have influenced grazer abundance through their effects on algae. For instance, some ephemeral algae preferentially attach to rugose, moisture-retaining barnacle tests (Farrell 1991), and microalgae may be more prevalent along the margins of moist barnacle beds as has been found for intertidal rock pools (Jackson et al. 2013). During the first summer and fall of this study, the green filamentous *Ulothrix* sp. dominated bare tiles. As *Ulothrix* sp. declined towards the end of summer, other algal species, predominantly foliose green, red, and brown ephemeral algae, attached to barnacle tests became more prevalent, a pattern found in past studies in this region (Kordas et al. 2017). While algal cover was quantitatively similar in both temperature treatments during the first year, its temporal dynamics differed; algal cover peaked later and declined more slowly within the warm treatment. High temperatures have highly variable interspecific effects on algae (Kordas et al., 2017, Wahl et al., 2021). *Ulothrix* sp. may have persisted during late summer due to greater growth under warm conditions or because barnacles, which can compete with algae for space or harbour populations of voracious grazers (Hesketh et al. 2021), were less abundant. On adjacent bedrock, *Ulothrix* sp. was most commonly observed in bare, log-damaged patches within barnacle beds, supporting an indirect negative effect of barnacles on this species (as has been documented with the ephemeral green alga *Urospora* spp.; Harley 2006). Meanwhile, barnacles can support the growth of other algae (such as *Pyropia* sp. and *Ulva* sp. seen here) by providing refuge from desiccation and grazing for algal spores and germlings (Geller 1991). Thus, algal cover may have been higher in the warm-cool treatment during the second year of the experiment because shifting thermal

536 conditions created a heterogenous mixture of bare space and sparse barnacles, allowing for the
537 growth of both heat-tolerant, barnacle-phobic species and heat-intolerant, barnacle-philic species.
538 The alpha diversity of tile communities generally increased as succession took its course,
539 tending to reach a minimum at the end of summer and a peak in winter each year, particularly
540 within cool treatments, as has been found in past studies (Kordas et al. 2015, Kordas et al. 2017).
541 Barnacle recruits, followed by opportunistic ephemeral algae, appeared shortly after bare
542 settlement tiles were installed, consistent with studies involving intertidal disturbance and
543 succession in the northeast Pacific (Farrell 1991, Geller 1991). Because barnacles act both as
544 facilitators (Farrell 1991) and food sources (Connell 1961), their presence allowed grazers (e.g.,
545 gastropods, amphipods, isopods, polychaete worms), predators (e.g., ribbon worms, barnacle-
546 eating flies), and secondary successional species (e.g., perennial algae; Farrell 1991) to move
547 into the nascent community. Thus, the higher alpha diversity observed in cool compared to warm
548 treatments may have indirectly resulted from facilitation by barnacles, been driven by more
549 species surviving under thermally benign conditions, or — more likely — have been produced
550 by a mixture of these two mechanisms. Disentangling these direct and indirect effects is
551 challenging given the experimental design employed.
552 We found that — contrary to our expectation — warming during the first summer of our
553 study did not make communities more susceptible to subsequent warming. Abiotic stressors can
554 enhance sensitivity to subsequent stressors; for instance, high temperatures can have more
555 detrimental effects on organisms previously exposed to thermal challenges (Siegle et al. 2018,
556 Samuels et al. 2021, Barker et al. 2021). Stress experienced during the early stages of community
557 assembly can shape community structure (e.g., Kreyling et al. 2011, Brown et al. 2018), with
558 effects continuing well after stress has subsided (Bjerke et al. 2017, Roos et al. 2020). In this

559 study, warming during the first summer resulted in persistent negative effects on grazer
560 abundance and community diversity a year or more later, likely mediated through differences in
561 barnacle abundance. Because foundation species (barnacle) cover was lower within the warm
562 compared to cool treatments after the first year, we anticipated that the effects of warming would
563 be magnified during the second year . Other studies have found that larger intertidal foundation
564 species are able to improve the survival, growth, and diversity of associated species in the face of
565 thermal stress (*Tetraclita japonica*, Cartwright and Williams 2014; *Mytilus californianus*,
566 Jurgens et al. 2022; *Semibalanus cariosus*; Hesketh and Harley 2023). Here, we found no such
567 effects; instead, warming in the second summer exerted a similar negative effect whether
568 warming had or had not occurred during prior year. The size and density of foundation species
569 can affect their facilitative ability, as has been found for high alpine cushion plants (Yang et al.
570 2017) and intertidal cordgrass (Irving and Bertness 2009). The small size of these acorn barnacle
571 species may prevent them from effectively buffering against warming (Rickards and Boulding
572 2015), even as they facilitate a speciose community (Harley 2006; Hesketh et al. 2021).
573 While intertidal systems are resilient up to a point, repeated atmospheric warming
574 threatens to disrupt even these historically stalwart communities (Menge et al. 2022). Our results
575 suggest that even for barnacle bed communities, known for their high turnover rate and resilience
576 (Conway-Cranos 2012), warming generates lasting effects on community structure due to
577 reductions in barnacle density and recruitment. As mean temperatures increase with climate
578 change, so, too, may thermal variability (Oliver et al. 2018; Perkins-Kirkpatrick and Lewis
579 2020). This variability increases the probability that critical thermal maxima are surpassed
580 (Kingsolver et al. 2013; Vasseur et al. 2014) and may accelerate shifts in ecological communities
581 (Harris et al. 2018). Climate change also encompasses multiple stressors beyond temperature,

and these may co-occur and interact with warming (Bible et al. 2017, MacLennan and Vinebrooke 2021). To understand the full risk of climate change to ecological communities, we must embrace complexity, integrating stochasticity, considering the temporal dimensions of stress, and otherwise seeking to emulate natural processes within our experimental designs.

References

Agrawal, A. and Jurgens, L. J. 2023. Effects of Asynchronous Stressors on the Eastern Oyster (*Crassostrea virginica*). - Estuaries and Coasts 46: 697–706.

Barker, C., Monaco, C. and McQuaid, C. 2021. Exposure to fluctuating temperature increases thermal sensitivity in two lineages of the intertidal mussel *Perna perna*. – Marine Ecology Progress Series 668: 85–95.

Barnes, M. 2000. The use of intertidal barnacle shells. - In: Oceanography and Marine Biology: an Annual Review - Taylor & Francis, pp. 157–187.

Bates, D., Mächler, M., Bolker, B. and Walker, S. 2015. Fitting linear mixed-effects models using lme4. - Journal of Statistical Software 67: 1–48.

Bible, J. M., Cheng, B. S., Chang, A. L., Ferner, M. C., Wasson, K., Zabin, C. J., Latta, M., Sanford, E., Deck, A. and Grosholz, E. D. 2017. Timing of stressors alters interactive effects on a coastal foundation species. - Ecology 98: 2468–2478.

Bjelde, B. E. and Todgham, A. E. 2013. Thermal physiology of the fingered limpet *Lottia digitalis* under emersion and immersion. - Journal of Experimental Biology 216: 2858–2869.

Bjerke, J. W., Bokhorst, S., Callaghan, T. V. and Phoenix, G. K. 2017. Persistent reduction of segment growth and photosynthesis in a widespread and important sub-Arctic moss species after cessation of three years of experimental winter warming. - Functional Ecology 31: 127–134.

Bozinovic, F., Cavieres, G., Martel, S. I., Alruiz, J. M., Molina, A. N., Roschzttardtz, H. and Rezende, E. L. 2020. Thermal effects vary predictably across levels of organization: empirical results and theoretical basis. - Proceedings of the Royal Society B: Biological Sciences 287: 20202508.

Brooks, M.E., Kristensen, K., van Benthem, K.J., Magnusson, A., Berg, C.W., Nielsen, A., Skaug, H.J., Maechler, M. and Bolker, B.M. 2017. glmmTMB balances speed and

flexibility among packages for zero-inflated generalized linear mixed modeling. The R Journal 9: 378-400

Brooks, P. R. and Crowe, T. P. 2019. Combined effects of multiple stressors: New insights into the influence of timing and sequence. – Frontiers in Ecology and Evolution. 7: 387.

Brown, N. E. M., Bernhardt, J. R., Anderson, K. M. and Harley, C. D. G. 2018. Increased food supply mitigates ocean acidification effects on calcification but exacerbates effects on growth. - Scientific Reports 8: 9800.

Bruno, J. F., Stachowicz, J. J. and Bertness, M. D. 2003. Inclusion of facilitation into ecological theory. - Trends in Ecology & Evolution 18: 119–125.

Buckley, L. B., Huey, R. B. and Kingsolver, J. G. 2022. Asymmetry of thermal sensitivity and the thermal risk of climate change. - Global Ecology and Biogeography 31: 2231–2244.

Bulleri, F., Bruno, J. F., Silliman, B. R. and Stachowicz, J. J. 2016. Facilitation and the niche: implications for coexistence, range shifts and ecosystem functioning. - Functional Ecology 30: 70–78.

Burrows, M. T., Hawkins, S. J., Moore, J. J., Adams, L., Sugden, H., Firth, L. and Mieszkowska, N. 2020. Global-scale species distributions predict temperature-related changes in species composition of rocky shore communities in Britain. - Global Change Biology 26: 2093–2105.

Cartwright, S. R. and Williams, G. A. 2014. How hot for how long? The potential role of heat intensity and duration in moderating the beneficial effects of an ecosystem engineer on rocky shores. - Marine Biology 161: 2097–2105.

Chim, C. K., Wong, H. P.-S. and Tan, K. S. 2016. *Tetraclita* (Cirripedia, Thoracica) tests as an important habitat for intertidal isopods and other marine and semi-terrestrial fauna on tropical rocky shores. - Crustaceana 89: 985–1040.

Christiansen, D. M., Iversen, L. L., Ehrlén, J. and Hylander, K. 2022. Changes in forest structure drive temperature preferences of boreal understorey plant communities. - Journal of Ecology 110: 631–643.

Connell, J. H. 1961. Effects of competition, predation by *Thais lapillus*, and other factors on natural populations of the barnacle *Balanus balanoides*. - Ecological Monographs 31: 61–104.

Conway-Cranos, L. L. 2012. Geographic variation in resilience: an experimental evaluation of four rocky intertidal assemblages. - Marine Ecology Progress Series 457: 67–83.

Creese, R. G. 1982. Distribution and abundance of the acmaeid limpet, *Patelloida latistrigata*, and its interaction with barnacles. - Oecologia 52: 85–96.

Dal Bello, M., Rindi, L. and Benedetti-Cecchi, L. 2019. Temporal clustering of extreme climate events drives a regime shift in rocky intertidal biofilms. - Ecology 100: e02578.

Dayton, P. K. 1971. Competition, disturbance, and community organization: the provision and subsequent utilization of space in a rocky intertidal community. - Ecological Monographs 41: 351–389.

Demes, K. W., Kordas, R. L. and Jorve, J. P. 2012. Ferry wakes increase seaweed richness and abundance in a sheltered rocky intertidal habitat. - Hydrobiologia 693: 1–11.

Ellison, A. M. 2019. Foundation species, non-trophic interactions, and the value of being common. - iScience 13: 254–268.

Farrell, T. M. 1991. Models and mechanisms of succession: An example from a rocky intertidal community. - Ecological Monographs 61: 95–113.

Fisheries and Oceans Canada. 2022. Tides, currents, and water levels. https://tides.gc.ca/en.

Fox, J. and Weisberg, S. 2019. An {R} companion to applied regression, third edition. Thousand Oaks CA: Sage.

Garrity, S. D. 1984. Some adaptations of gastropods to physical stress on a tropical rocky shore. - Ecology 65: 559–574.

Geller, J. B. 1991. Gastropod grazers and algal colonization on a rocky shore in northern California: the importance of the body size of grazers. - Journal of Experimental Marine Biology and Ecology 150: 1–17.

Gilman, S. E. and Rognstad, R. L. 2018. Influence of food supply and shore height on the survival and growth of the barnacle *Balanus glandula* (Darwin). - Journal of Experimental Marine Biology and Ecology 498: 32–38.

Gilman, S., Hayford, H., Craig, C. and Carrington, E. 2015. Body temperatures of an intertidal barnacle and two whelk predators in relation to shore height, solar aspect, and microhabitat. - Marine Ecology Progress Series 536: 77–88.

Gutiérrez, J. L., Bagur, M., Lorenzo, R. A. and Palomo, M. G. 2023. A facultative mutualism between habitat-forming species enhances the resistance of rocky shore communities to heat waves. – Frontiers in Ecology and Evolution 11: 1278762.

Hamilton, H. and Gosselin, L. 2020. Ontogenetic shifts and interspecies variation in tolerance to desiccation and heat at the early benthic phase of six intertidal invertebrates. - Marine Ecology Progress Series 634: 15–28.

Hammill, E. and Dart, R. 2022. Contributions of mean temperature and temperature variation to population stability and community diversity. - Ecology and Evolution 12: e8665.

680 Harley, C. D. G. 2006. Effects of physical ecosystem engineering and herbivory on intertidal
681 community structure. - Marine Ecology Progress Series 317: 29–39.

682 Harley, C. 2008. Tidal dynamics, topographic orientation, and temperature-mediated mass
683 mortalities on rocky shores. - Marine Ecology Progress Series 371: 37–46.

684 Harley, C. D. G. 2011. Climate change, keystone predation, and biodiversity loss. - Science 334:
685 1124–1127.

686 Harley, C. D. G. and O'Riley, J. L. 2011. Non-linear density-dependent effects of an intertidal
687 ecosystem engineer. - Oecologia 166: 531–541.

688 Harris, R. M. B., Beaumont, L. J., Vance, T. R., Tozer, C. R., Remenyi, T. A., Perkins-
689 Kirkpatrick, S. E., Mitchell, P. J., Nicotra, A. B., McGregor, S., Andrew, N. R., Letnic,
690 M., Kearney, M. R., Wernberg, T., Hutley, L. B., Chambers, L. E., M-S, F., Keatley, M.
691 R., Woodward, C. A., Williamson, G., Duke, N. C., and Bowman, D. M. J. S. 2018.
692 Biological responses to the press and pulse of climate trends and extreme events. - Nature
693 Climate Change 8: 579–587.

694 Hartig, F. 2021. DHARMa: Residual diagnostics for hierarchical (multi-level/mixed) regression
695 models. R package version 0.4.6.

696 He, Q., Bertness, M. D. and Altieri, A. H. 2013. Global shifts towards positive species
697 interactions with increasing environmental stress. - Ecology Letters 16: 695–706.

698 Helmuth, B., Broitman, B. R., Blanchette, C. A., Gilman, S., Halpin, P., Harley, C. D. G.,
699 O'Donnell, M. J., Hofmann, G. E., Menge, B. and Strickland, D. 2006. Mosaic patterns
700 of thermal stress in the rocky intertidal zone: Implications for climate change. -
701 Ecological Monographs 76: 461–479.

702 Hesketh, A. V. and Harley, C. D. G. 2023. Extreme heatwave drives topography-dependent
703 patterns of mortality in a bed-forming intertidal barnacle, with implications for associated
704 community structure. - Global Change Biology 29: 165–178.

705 Hesketh, A. V., Schwindt, E. and Harley, C. D. G. 2021. Ecological and environmental context
706 shape the differential effects of a facilitator in its native and invaded ranges. - Ecology
707 102: e03478.

708 IPCC. 2023. Climate Change 2023: Synthesis Report. Contribution of Working Groups I, II and
709 III to the Sixth Assessment Report of the Intergovernmental Panel on Climate Change
710 (Core Writing Team, Lee, H. and Romero, J., Eds.) - IPCC, Geneva, Switzerland, pp. 35–
711 115.

712 Irving, A. D., Bertness, M. D. 2009. Trait-dependent modification of facilitation on cobble
713 beaches. - Ecology 90: 3042–3050.

714 Jackson, A. C., Murphy, R. J. and Underwood, A. J. 2013. Biofilms on rocky shores: Influences
715 of rockpools, local moisture and temperature. - Journal of Experimental Marine Biology
716 and Ecology 443: 46–55.

717 Jackson, M. C., Pawar, S. and Woodward, G. 2021. The temporal dynamics of multiple stressor
718 effects: From individuals to ecosystems. - Trends in Ecology & Evolution 36: 402–410.

719 Jurgens, L. J., Ashlock, L. W. and Gaylord, B. 2022. Facilitation alters climate change risk on
720 rocky shores. – Ecology 103: e03596.

721 Kindt, R. and Coe, R. 2005. Tree diversity analysis. A manual and software for common
722 statistical methods for ecological and biodiversity studies. Nairobi: World Agroforestry
723 Centre (ICRAF).

724 Kingsolver, J. G., Diamond, S. E. and Buckley, L. B. 2013. Heat stress and the fitness
725 consequences of climate change for terrestrial ectotherms. - Functional Ecology 27:
726 1415–1423.

727 Kordas, R. and Harley, C. 2016. Demographic responses of coexisting species to *in situ*
728 warming. - Marine Ecology Progress Series 546: 147–161.

729 Kordas, R. L., Dudgeon, S., Storey, S. and Harley, C. D. G. 2015. Intertidal community
730 responses to field-based experimental warming. - Oikos 124: 888–898.

731 Kordas, R. L., Donohue, I. and Harley, C. D. G. 2017. Herbivory enables marine communities to
732 resist warming. - Science Advances 3: e1701349.

733 Kreyling, J., Jentsch, A. and Beierkuhnlein, C. 2011. Stochastic trajectories of succession
734 initiated by extreme climatic events. - Ecology Letters 14: 758–764.

735 LaScala-Gruenewald, D. E. and Denny, M. W. 2020. Long-term mechanistic hindcasts predict
736 the structure of experimentally-warmed intertidal communities. - Oikos 129: 1645–1656.

737 Lee, R. H., Morgan, B., Liu, C., Fellowes, J. R. and Guénard, B. 2021. Secondary forest
738 succession buffers extreme temperature impacts on subtropical Asian ants. - Ecological
739 Monographs 91: e01480.

740 Lenth, R. 2023. emmeans: Estimated marginal means, aka least-squares means. R package
741 version 1.8.6, https://CRAN.R-project.org/package=emmeans.

742 Little, C. 1989. Factors governing patterns of foraging activity in littoral marine herbivorous
743 molluscs. – Journal of Molluscan Studies 55: 273–284.

744 Little, C., Trowbridge, C. D., Williams, G. A., Hui, T. Y., Pilling, G. M., Morritt, D. and Stirling,
745 P. 2021. Response of intertidal barnacles to air temperature: Long-term monitoring and
746 *in-situ* measurements. - Estuarine, Coastal and Shelf Science 256: 107367.

747 Liversage, K., Kotta, J., Fraser, C. M. L., Figueira, W. F. and Coleman, R. A. 2020. The
748 overlooked role of taphonomy in ecology: post-mortem processes can outweigh
749 recruitment effects on community functions. - Oikos 129: 420–432.

750 Ma, C.-S., Wang, L., Zhang, W. and Rudolf, V. H. W. 2018. Resolving biological impacts of
751 multiple heat waves: interaction of hot and recovery days. - Oikos 127: 622–633.

752 MacLennan, M. M. and Vinebrooke, R. D. 2021. Exposure order effects of consecutive stressors
753 on communities: the role of co-tolerance. - Oikos 130: 2111–2121.

754 Marshall, K. E. and Sinclair, B. J. 2015. The relative importance of number, duration and
755 intensity of cold stress events in determining survival and energetics of an overwintering
756 insect. - Functional Ecology 29: 357–366.

757 Menge, B. A., Gravem, S. A., Johnson, A., Robinson, J. W. and Poirson, B. N. 2022. Increasing
758 instability of a rocky intertidal meta-ecosystem. - Proc. Natl. Acad. Sci. U.S.A. 119:
759 e2114257119.

760 Montie, S. and Thomsen, M. S. 2023. Long-term community shifts driven by local extinction of
761 an iconic foundation species following an extreme marine heatwave. - Ecology and
762 Evolution 13: e10235.

763 Ober, G., Rognstad, R. and Gilman, S. 2019. The cost of emersion for the barnacle *Balanus*
764 *glandula*. - Marine Ecology Progress Series 627: 95–107.

765 Oliver, E. C. J., Donat, M. G., Burrows, M. T., Moore, P. J., Smale, D. A., Alexander, L. V.,
766 Benthuysen, J. A., Feng, M., Sen Gupta, A., Hobday, A. J., Holbrook, N. J., Perkins-
767 Kirkpatrick, S. E., Scannell, H. A., Straub, S. C. and Wernberg, T. 2018. Longer and
768 more frequent marine heatwaves over the past century. - Nature Communications 9:
769 1324.

770 Oksanen, J., Blanchet, F.G., Friendly, M., Kindt, R., Legendre, P., McGlinn, D., Minchin, P.R.,
771 O'Hara, R. B., Simpson, G.L., Solymos, P., Stevens, M.H.H., Szoecs, E. and Wagner, H.
772 2020. vegan: Community Ecology Package. R package version 2.6-4. https://CRAN.R-
773 project.org/package=vegan

774 Perkins-Kirkpatrick, S. E. and Lewis, S. C. 2020. Increasing trends in regional heatwaves. -
775 Nature Communications 11: 3357.

776 Qian, P.-Y. and Liu, L.-L. 1990. Recruitment of barnacles into empty adult tests. - Journal of
777 Experimental Marine Biology and Ecology 142: 63–74.

778 Raymond, W. W., Barber, J. S., Dethier, M. N., Hayford, H. A., Harley, C. D. G., King, T. L.,
779 Paul, B., Speck, C. A., Tobin, E. D., Raymond, A. E. T. and McDonald, P. S. 2022.
780 Assessment of the impacts of an unprecedented heatwave on intertidal shellfish of the
781 Salish Sea. - Ecology 103: e3798.

Reid, H. and Harley, C. 2021. Low temperature exposure determines performance and thermal microhabitat use in an intertidal gastropod (*Littorina scutulata*) during the winter. - Mar. Ecol. Prog. Ser. 660: 105–118.

Reimer, A. A. 1976. Succession of invertebrates in vacant tests of *Tetraclita stalactifera panamensis*. – Marine Biology 35: 239–251.

Rickards, K. and Boulding, E. 2015. Effects of temperature and humidity on activity and microhabitat selection by *Littorina subrotundata*. - Marine Ecology Progress Series 537: 163–173.

Roos, R. E., Birkemoe, T., Asplund, J., Ľuptáčik, P., Raschmanová, N., Alatalo, J. M., Olsen, S. L. and Klanderud, K. 2020. Legacy effects of experimental environmental change on soil micro-arthropod communities. - Ecosphere 11: e03030.

Rose, N. L., Yang, H., Turner, S. D. and Simpson, G. L. 2012. An assessment of the mechanisms for the transfer of lead and mercury from atmospherically contaminated organic soils to lake sediments with particular reference to Scotland, UK. - Geochimica et Cosmochimica Acta 82: 113–135.

Samuels, T., Rynearson, T. A. and Collins, S. 2021. Surviving heatwaves: Thermal experience predicts life and death in a Southern Ocean diatom. - Frontiers in Marine Science 8: 600343.

Scrosati, R. A. and Ellrich, J. A. 2016. A 12-year record of intertidal barnacle recruitment in Atlantic Canada (2005-2016): Relationships with sea surface temperature and phytoplankton abundance. - PeerJ 4: e2623–e2623.

Siegle, M. R., Taylor, E. B. and O'Connor, M. I. 2018. Prior heat accumulation reduces survival during subsequent experimental heat waves. - Journal of Experimental Marine Biology and Ecology 501: 109–117.

Siegle, M. R., Taylor, E. B. and O'Connor, M. I. 2022. Heat wave intensity drives sublethal reproductive costs in a tidepool copepod. - Integrative Organismal Biology 4: obac005.

Silva, A. C. F., Mendonça, V., Paquete, R., Barreiras, N. and Vinagre, C. 2015. Habitat provision of barnacle tests for overcrowded periwinkles. - Marine Ecology 36: 530–540.

Stickle, W. B., Carrington, E. and Hayford, H. 2017. Seasonal changes in the thermal regime and gastropod tolerance to temperature and desiccation stress in the rocky intertidal zone. - Journal of Experimental Marine Biology and Ecology 488: 83–91.

Sun, B., Jiang, M., Han, G., Zhang, L., Zhou, J., Bian, C., Du, Y., Yan, L. and Xia, J. 2022. Experimental warming reduces ecosystem resistance and resilience to severe flooding in a wetland. - Science Advances 8: eabl9526.

816 Tomanek, L. and Helmuth, B. 2002. Physiological ecology of rocky intertidal organisms: A
817 synergy of concepts. - Integrative and Comparative Biology 42: 771–775.

818 Uyà, M., Bulleri, F., Wright, J. T. and Gribben, P. E. 2020. Facilitation of an invader by a native
819 habitat-former increases along interacting gradients of environmental stress. - Ecology
820 101: e02961.

821 Vasseur, D. A., DeLong, J. P., Gilbert, B., Greig, H. S., Harley, C. D. G., McCann, K. S.,
822 Savage, V., Tunney, T. D. and O'Connor, M. I. 2014. Increased temperature variation
823 poses a greater risk to species than climate warming. – Proceedings of the Royal Society
824 B. 281: 20132612.

825 Vermeij, G. J. 1978. Biogeography and Adaptation: Patterns of Marine Life. - Harvard
826 University Press.

827 Wahl, M., Barboza, F. R., Buchholz, B., Dobretsov, S., Guy-Haim, T., Rilov, G., Schuett, R.,
828 Wolf, F., Vajedsamiei, J., Yazdanpanah, M. and Pansch, C. 2021. Pulsed pressure:
829 Fluctuating impacts of multifactorial environmental change on a temperate macroalgal
830 community. - Limnology and Oceanography 66: 4210–4226.

831 Weitzman, B., Konar, B., Iken, K., Coletti, H., Monson, D., Suryan, R., Dean, T., Hondolero, D.
832 and Lindeberg, M. 2021. Changes in rocky intertidal community structure during a
833 marine heatwave in the northern Gulf of Alaska. - Frontiers in Marine Science 8: 556820.

834 Wood, S. N. 2011. Fast stable restricted maximum likelihood and marginal likelihood estimation
835 of semiparametric generalized linear models. - Journal of the Royal Statistical Society
836 (B) 73: 3–36.

837 Wu, R. S.-S. 1981. The effect of aggregation on breeding in the barnacle *Balanus glandula*,
838 Darwin. - Canadian Journal of Zoology 59: 890–892.

839 Yang, Y., Chen, J.-G., Schöb, C. and Sun, H. 2017. Size-mediated interaction between a cushion
840 species and other non-cushion species at high elevations of the Hengduan Mountains, SW
841 China. – Frontiers in Plant Science 8: 465.

842

843

Appendix 1: Additional methodological details and results for 'The effect of single versus successive warm summers on an intertidal community'

Tile construction

Experimental tiles consisted of a sandwich of two 15 x 15 cm squares of high-density polyethylene "puckboard" (Redwood Plastics, BC, Canada). The bottom tile (white, 9.5 mm thickness) was used to anchor the tile assembly to the underlying bedrock using two 18-8 stainless steel lag bolts (6.35 mm x 3.81 cm; Pacific Fasteners, BC, Canada). The lag bolts were threaded through 0.95 cm holes (with a 1.91 cm counterbore) in the bottom tile unit and screwed into plastic anchors (6.35 mm x 3.81 cm High-Strength Twist-Resistant Plastic Anchors for Block and Brick; McMaster-Carr, IL, USA) set within 7.94 mm drilled holes in the bedrock below. The top tile unit (white or black, 6.4 mm thickness) was affixed to the bottom tile unit using four stainless steel button screws and tee nuts (6.35 mm size; Pacific Fasteners, BC, Canada), one in each corner of the tile assembly. Tee nuts were hammered into 9.5 mm holes in the bottom tile units, and button screws were threaded through 6.35 mm interior diameter stainless steel washers (Pacific Fasteners, BC, Canada) and corresponding 9.5 mm holes in the top tile units to facilitate assembly. A central 1.91 cm hole was drilled through the top tile to allow a temperature logger to be installed within the experimental tile unit. To enhance epoxy adhesion while constructing the settlement area, 12–5 mm holes were drilled within the central 6.9 x 6.9 cm area of the top tile unit, and this area was sanded. We placed a circle of cork within the central hole before spreading a thin layer (≤ 5 mm) of Sea Goin' Poxy Putty (Permalite Plastics, Rancho Dominguez, CA, USA) over the area. To enhance fine-scale heterogeneity of the surface, we pressed finely

ground Epsom salts into the putty. Once the epoxy dried, the Epsom salts were dissolved with tap water, leaving behind fine pock marks on the settlement surface, and the cork was removed from the central hole to create a cavity for the temperature logger. See Fig. A1 for a detailed diagram.

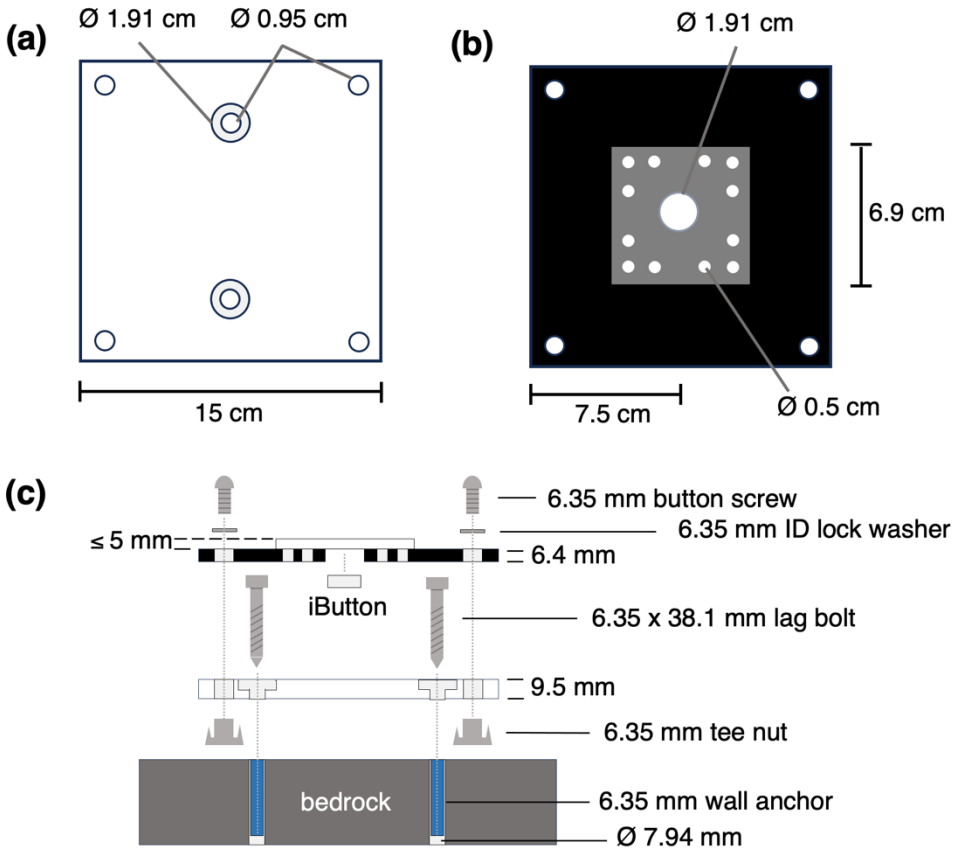

Figure A1. Diagrams of representative tile assembly used for testing the effect of artificial warming on barnacle bed communities. **(a)** Bottom unit of tile assembly, viewed from top without hardware installed. **(b)** Top unit of tile, in this case a black (warm) treatment tile, viewed from the top without hardware installed. The transparent square represents the central epoxy settlement area overlying the tile. **(c)** Exploded view of tile including hardware for assembly and installation, viewed from the side. ø = diameter, ID = interior diameter. The exact position of the holes, absent the central hole for the iButton temperature logger, was not measured, so these positions have been approximated from photographs.

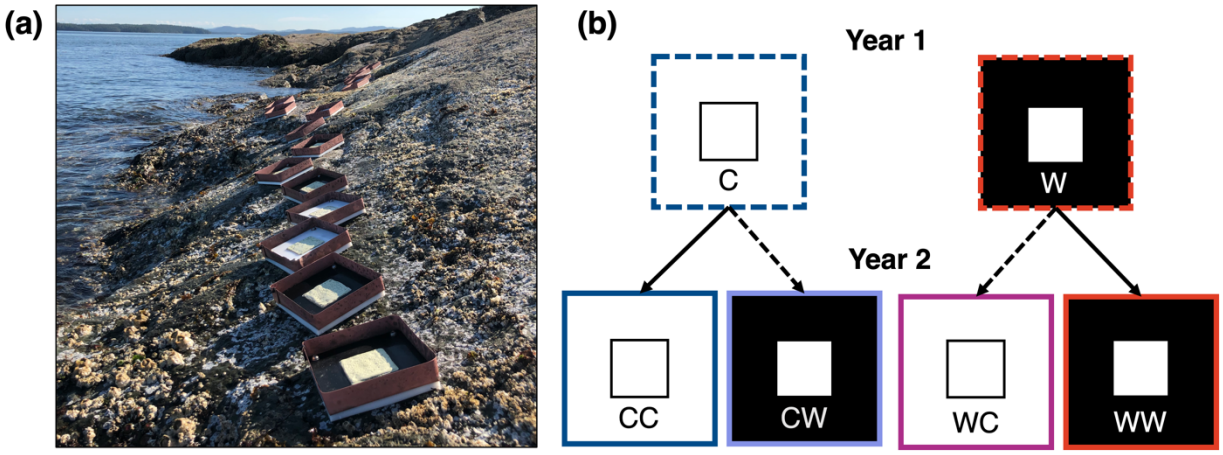

Figure A2. Experimental tiles and experimental design for testing how single versus successive warm summers affected intertidal barnacle bed communities at TESNO, EN, Salt Spring Island. **(a)** Photograph of experimental tiles anchored in the intertidal zone, still with copper fences attached to facilitate grazer manipulations. **(b)** Schematic of experimental design, wherein black (W=warm) and white (C=cool) settlement tiles were monitored for one year before swapping the treatment for half of each group of tiles (indicated by dashed arrows), generating four treatments for the second year of the study (CC = cool summer – cool summer; CW = cool summer – warm summer; WC = warm summer – cool summer; WW = warm summer – cool summer).

Changes to experimental design

In April 2019, we installed five blocks of 20 tiles each, half of which were white and half of which were black (N=100) at a shore level of 2.27 ± 0.06 m (mean ± SE) above Canadian chart datum. However, due to floating log disturbance within some of the blocks, several tiles were lost. In June 2019, we relocated tiles to more suitable areas to prevent log disturbance from causing further losses, expanding the experiment to six experimental blocks with approximately 16 tiles each, eight black and eight white where blocks were balanced (N=96). All tiles were re-installed at a similar shore level of 2.34 ± 0.07 m.

We originally intended to manipulate herbivore community diversity on the experimental tiles to test how grazer diversity influences resilience to warming, an effort that was ultimately abandoned due to the ineffectiveness of copper fences at controlling the abundance of some

species, thermal stress killing others, and frequent log disturbance crushing copper fences. From March–August 2019, copper fences were affixed around each experimental tile (0.511 mm thick, 3.8 cm high above the level of the tile; Fig. S1). Different combinations of grazers (using *Littorina sitkana*, *Littorina scutulata*, *Lottia digitalis*, and *Lottia paradigitalis*) were established on each tile: all four grazers, all three combinations of three grazers, each grazer alone, and no grazers. Despite the presence of copper fences, littorine snails — perhaps aided by wave action — were nonetheless readily able to move on and off of the tiles. A pivot to limpet-only treatment combinations (using both previously mentioned *Lottia* spp. and *Lottia scutum*) in June 2019 was also unsuccessful, as mortality in most limpet species was very high, likely due to thermal stress on the still relatively bare tiles. What limpets of these species did survive during this period were often found at the edges of tiles or wedged in the cracks between the tile and copper fence, and thus their biological function within tile communities was likely minimal. In August 2019, we thus removed the copper fences, and herbivores of all species were allowed unfettered access to tile communities thereafter.

Table A1. Design iterations employed during study of passive summertime warming on barnacle bed communities at TESNO, EN. Treatments were applied from initial establishment in March 2019 to the experiment endpoint in February 2021.

Iteration	Time period	Manipulations	Treatments	Blocks	n	Reason for change
1	April–June 2019	Temperature · herbivory (2 limpets + 2 littorines)	2 · 10 = 20	5	5	Littorine movement
2	June–August 2019	Temperature · herbivory (3 limpet spp.)	2 · 8 = 16	6	6	Log disturbance, thermal stress
3	August 2019–February 2021	Temperature · time	2 · 2 = 4	6	24	

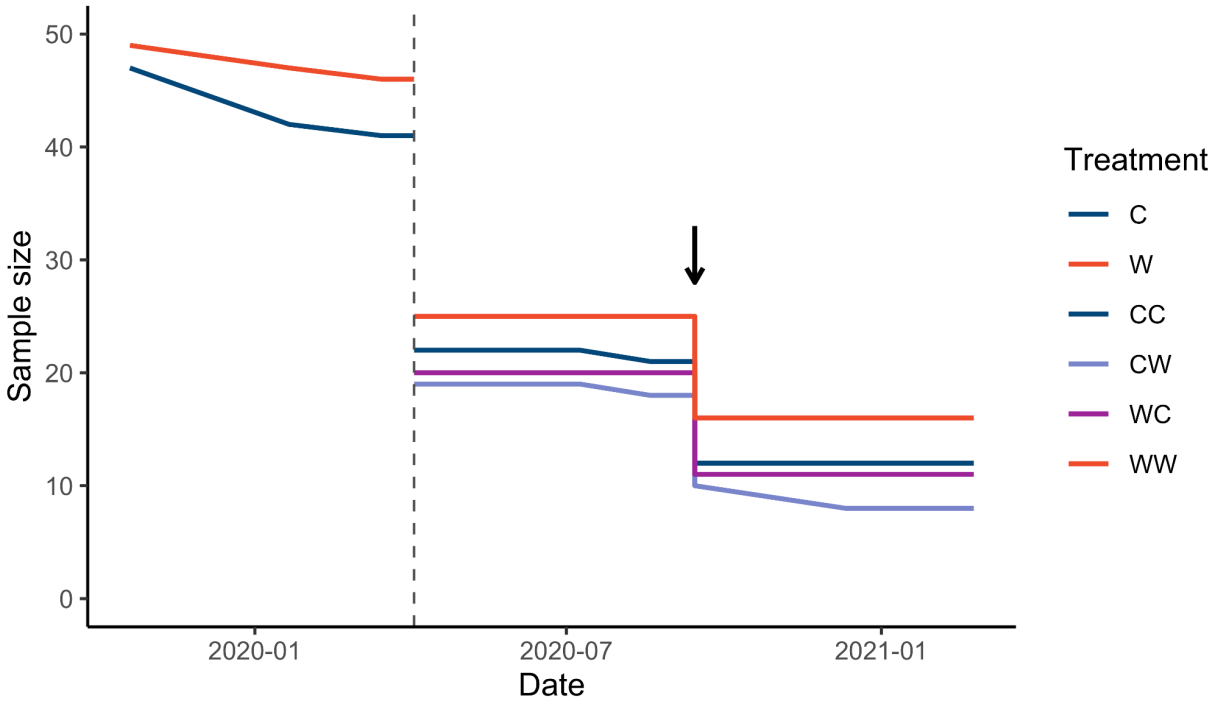

Figure A3. Changes in the number of experimental tiles within treatment groups over time. The time series begins after the end of early herbivore manipulations. The dashed vertical line indicates when year two tile treatments (CC, CW, WC, WW) were established by reversing the color of half of the tiles, at which point sample sizes were effectively halved, and the arrow indicates when the first set of tiles was destructively sampled to measure epifaunal abundance and community structure in September 2020. See Fig. A2 for treatment abbreviations.

Estimating tile shore levels

Shore levels for individual tiles were estimated from temperature traces and tide data (Fisheries and Oceans Canada, 2022). For each tile, temperature data from spring low tide series during the middle of summer were manually searched for three intervals where temperatures clearly transitioned from moderate sea surface temperatures one hour (typically ~12–15 ºC) to much higher aerial temperatures (>20 ºC) the next. These transitions occur when tiles become emersed after being immersed. The shore level of the tile above Canadian chart datum was approximated as the mean level of the tide between those two timepoints. These shore level values were subsequently used in filtering temperature data for plotting and analyses.

Additional temperature data

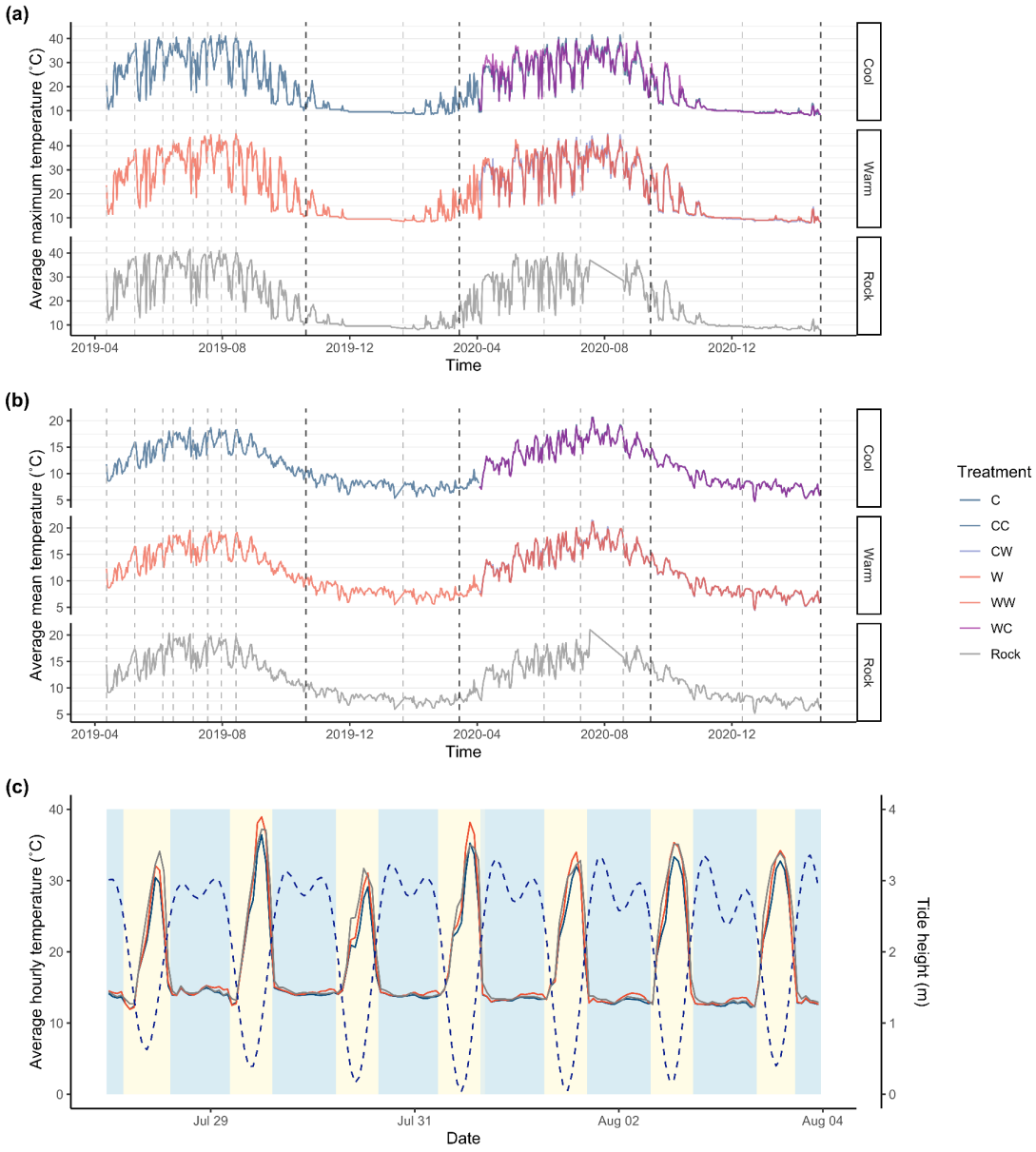

Figure A4. Temperatures of experimental tile and adjacent bedrock, as recorded by iButton temperature loggers during a two-year passive warming experiment at TESNO¸EN, Salt Spring Island. **(a)** Mean daily maximum and **(b)** mean temperatures over the entire experiment, averaged for each treatment. Dashed vertical lines represent when visual surveys were performed, with darker lines representing data for which post-summer and post-winter analyses were conducted. **(c)** Hourly temperature data collected between 28 July 2019 and 4 August 2019 averaged among all tiles in each treatment. Tide data are overlaid (height above Canadian chart datum; dashed line) to illustrate the effect of emersion (pale yellow background) and submersion (pale blue background). Treatment abbreviations as in Fig. A2.

Warm treatments had higher mean temperatures than cool treatments in both year one ($F_{2,73} = 15.58$, $p < 0.001$) and year two ($F_{4,67} = 10.08$, $p < 0.001$). As with mean daily maximum temperature, the mean bedrock temperature was more similar to the warm treatment during the first year and more similar to the cool treatments in the second year (Appendix 2: Table A10). The maximum temperature reached within the warm treatment was higher than bedrock and the cool treatment during both year one ($F_{2,77} = 33.46$, $p < 0.001$) and year two ($F_{4,67} = 9.36$, $p < 0.001$; Appendix 2: Tables A14).

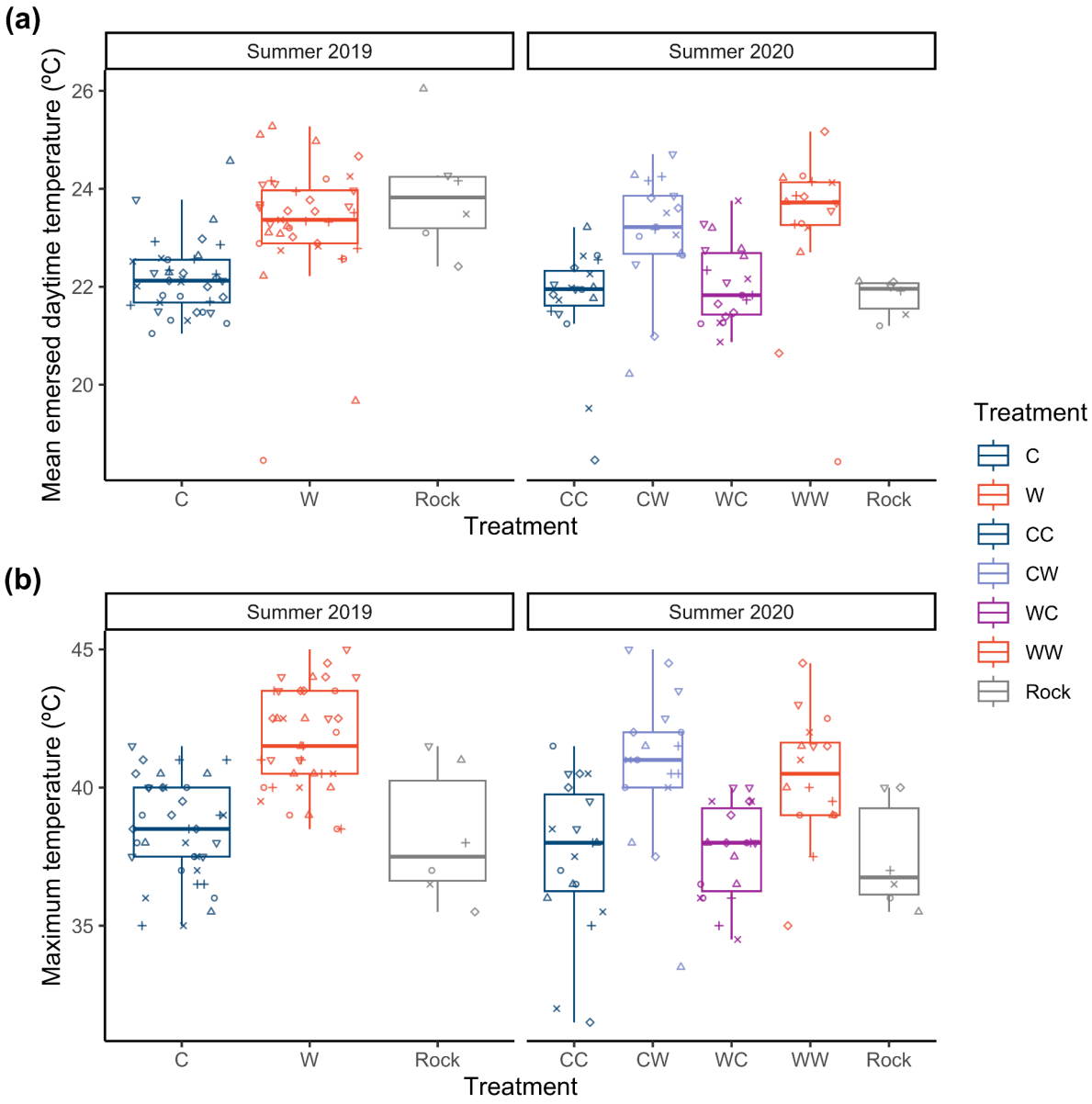

Figure A5. Differences in **(a)** mean emersed daytime substratum temperatures and **(b)** maximum temperatures of experimental tiles and adjacent bedrock recorded by embedded temperature loggers at TESNO ̓EN, Salt Spring Island. Points represent the mean value for each of the six experimental blocks, using only temperatures collected during daytime summer low tides between 15 June – 31 August. The exact number of temperature loggers recording data varied among treatments and over time. Treatment abbreviations as in Fig. A2.

Additional biological data

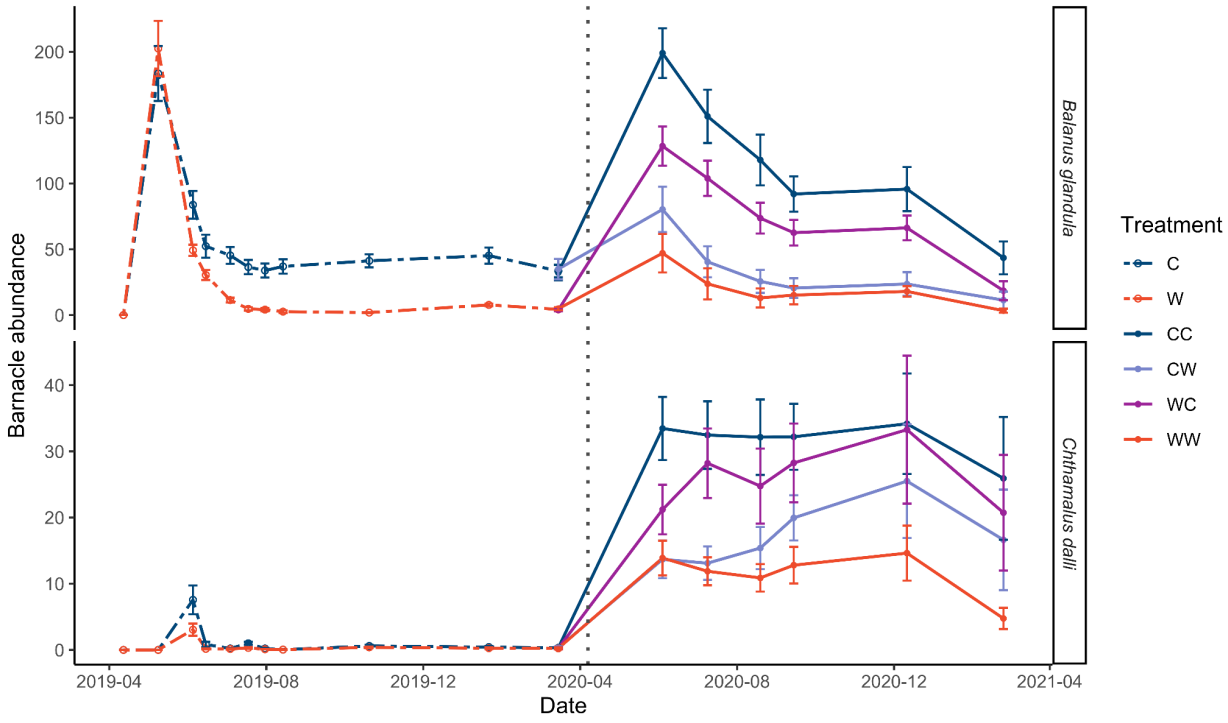

Figure A6. Mean abundance of *Balanus glandula* and *Chthamalus dalli* acorn barnacles on experimental tiles at TESNO, EN, including recruits, over the course of the entire experiment. Error bars represent standard errors about the mean. The dotted line represents the time at which experimental treats were switched from those of Year 1 to Year 2. Note that y axes are on different scales. Treatment abbreviations as in Fig. A2.

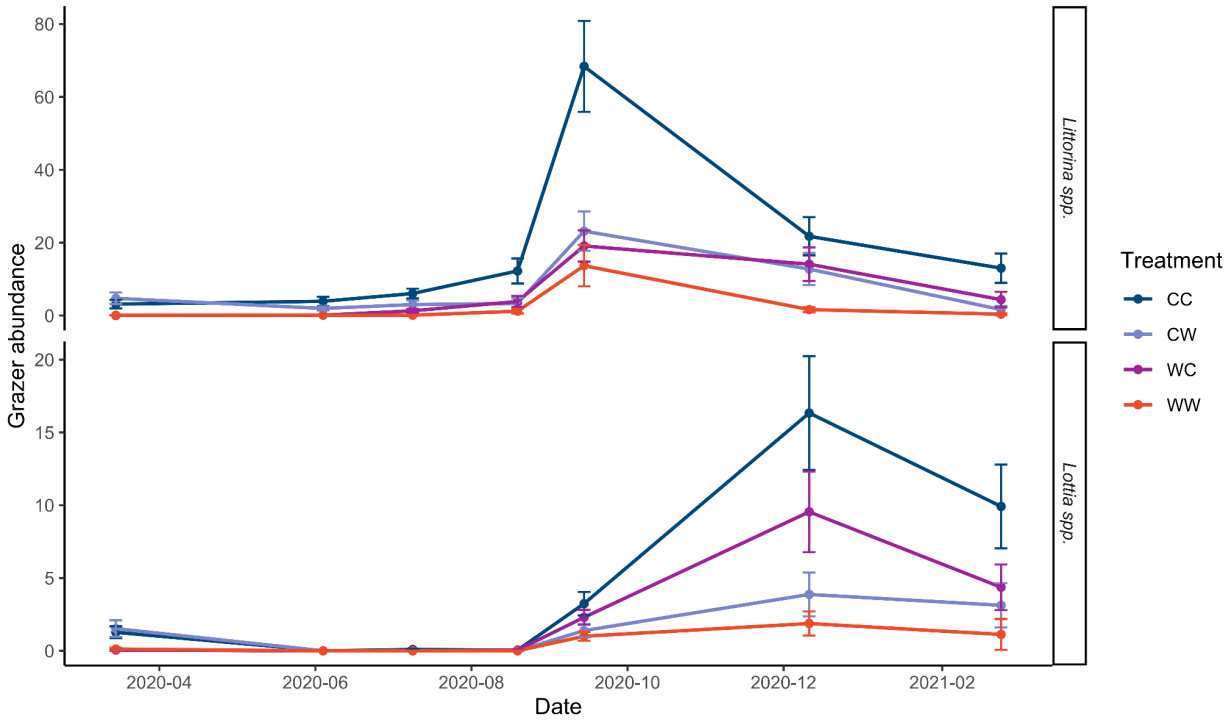

Figure A7. Mean abundance of *Lottia* spp. and *Littorina spp.* gastropod grazers on experimental tiles at TESNO, EN, including recruits, over the course of the entire experiment. Error bars represent standard errors about the mean. Note that y axes are on different scales. Treatment abbreviations as in Fig. A2.

Temporal patterns in invertebrate Shannon diversity mirrored patterns in overall species richness; diversity remained low in the first year, exhibited a peak in fall of the second year, and gradually declined thereafter (Fig. A8b). In the first year, the negative effect of warming on Shannon diversity was more apparent in late winter compared to post-summer (Fig. A9a; Type III ANOVA; $\chi^2_1 = 13.01$, $p < 0.001$). In the second year, invertebrate Shannon diversity was higher post-summer than during winter (Type III ANOVA; $\chi^2_1 = 41.80$, $p < 0.001$), and treatments that were warmed during the first year (WC and WW) had significantly lower Shannon diversity than their comparatively cool counterparts ($\chi^2_1 = 9.37$, $p = 0.00220$). Warming during the second year (CW and WW) exerted a negative, though marginally insignificant, effect on Shannon diversity (treatment_{y1}: $\chi^2_1 = 3.69$, $p = 0.0546$). Tukey-Kramer *post hoc* tests showed

that the successively warm treatment (WW) had substantially lower algal cover than the successively cool treatment (CC) and the warm–cool treatment (WC), but not the cool–warm treatment (CW).

Algal Shannon diversity was highest in winter, and cover became low and sometimes nonexistent from late summer to early fall (Fig. A8c). Where temperatures were cooler during the first year of the experiment, algal cover was higher (Fig. A9c), leading to a significant negative effect of warming (Type II ANOVA; $\chi^2 = 14.01$, $p < 0.001$). In the second year of the experiment, algal cover (and thus diversity) was negligible over the summer and was highly variable within treatment groups at the end of the winter. Warming, whether applied during the first or second year, did not exert a significant effect on algal Shannon diversity.

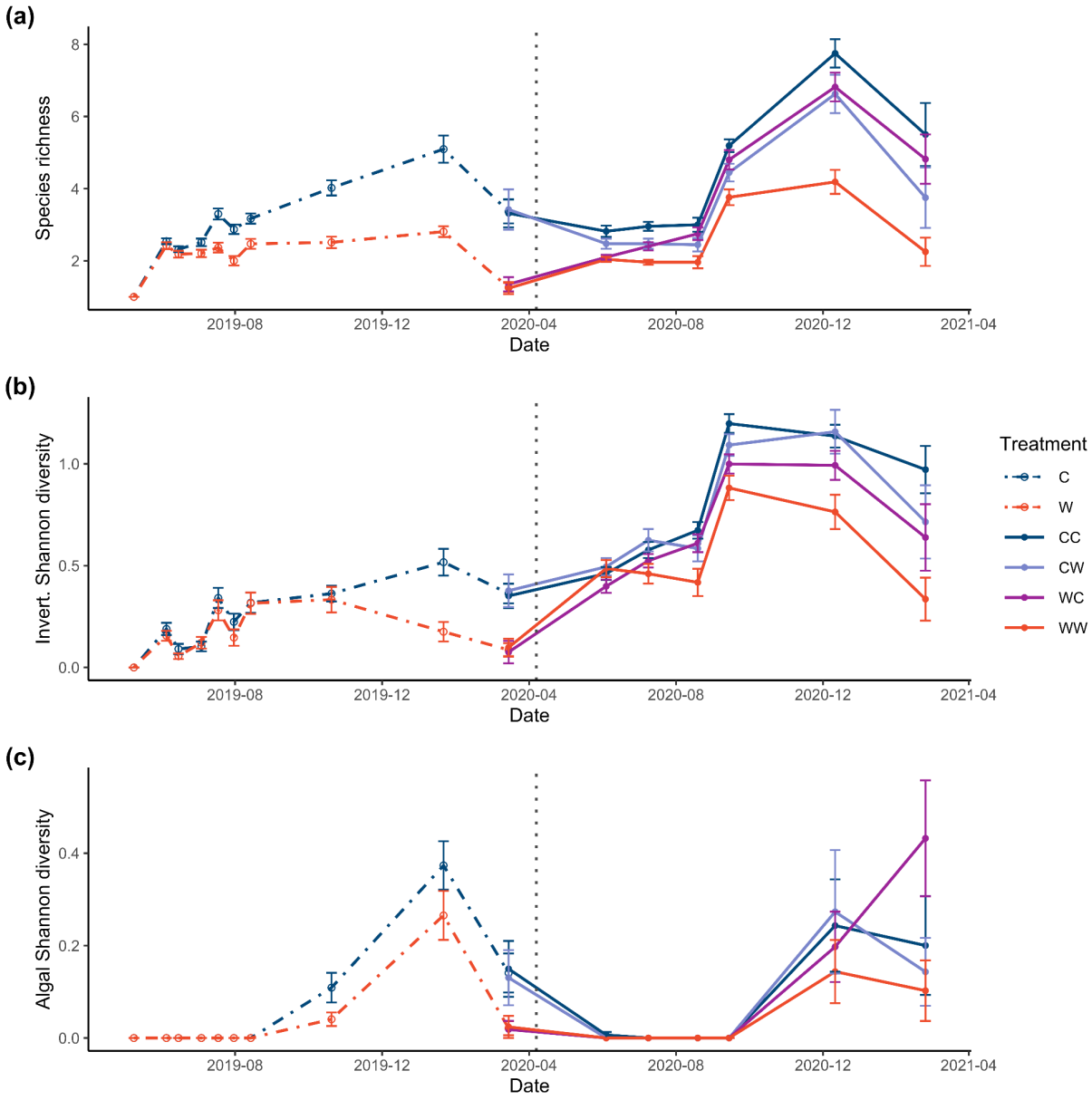

Figure A8. The effect of temperature treatments on alpha diversity of experimental communities over time, as described by changes in the **(a)** species richness of whole tile communities and Shannon diversity of **(b)** the invertebrate community and **(c)** the algal community. Error bars represent standard errors about the mean. The dotted vertical line represents the time at which experimental treatments were switched from those of Year 1 to Year 2. Note that y axes are on different scales. Treatment abbreviations as in Fig. A2.

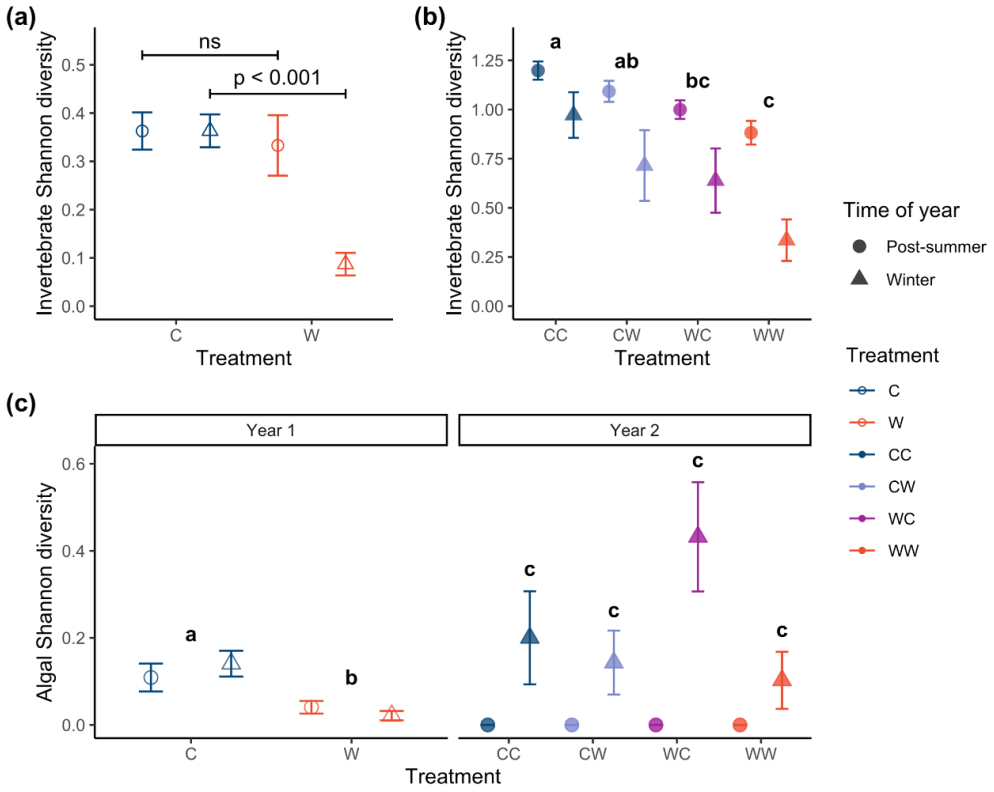

Figure A9. Shannon diversity of the **(a)** invertebrate community during the first year, **(b)** invertebrate community during the second year, and **(c)** algal community during the entire two-year passive warming experiment at TESNO, EN. Samples were obtained through visual surveys. Error bars represent standard error about the mean. Differences between treatment groups, as determined using Tukey-Kramer *post hoc* tests, are indicated through brackets (ns = non-significant) or lowercase letters. Treatment abbreviations as in Fig. A2.

The richness and Shannon diversity of destructively sampled tile epifaunal communities were also examined (Fig. A10). Richness was similar between sampling timepoints, but warming applied during the second summer had a negative effect on epifaunal richness (Type III ANOVA; $\chi^2_1 = 5.69$, $p = 0.0171$), while warming applied during the second summer had a persistent negative effect ($treatment_{y1}$: $\chi^2_1 = 3.91$, $p = 0.0480$). Trends in Shannon diversity were analogous; warming had both contemporaneous ($\chi^2_1 = 15.49$, $p = 0.001$), and persistent negative effects on the Shannon diversity of the epifaunal community ($treatment_{y1}$: $\chi^2_1 = 12.87$, $p = 0.001$).

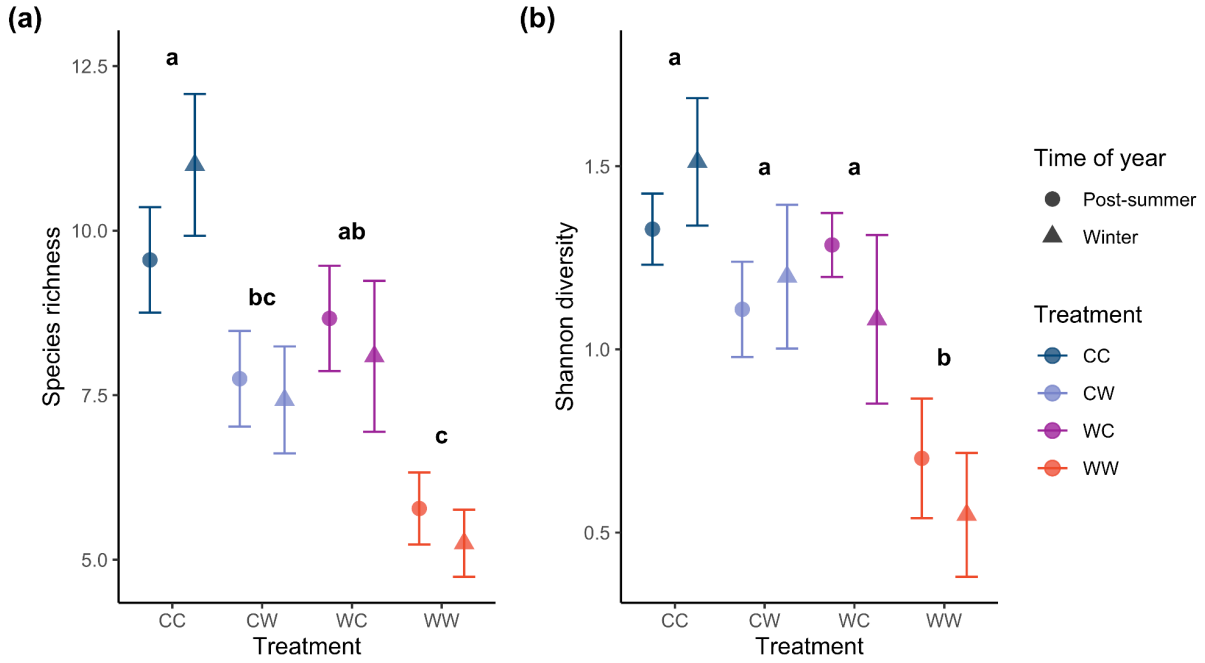

Figure A10. (a) Species richness and **(b)** Shannon diversity of epifaunal community within destructively sampled experimental tiles in the second year of a multi-year passive warming experiment at TESNO, EN. Error bars represent standard error about the mean. Differences between treatment groups, as determined using Tukey-Kramer *post hoc* tests, are indicated using lowercase letters. Treatment abbreviations as in Fig. A2.

Changes in community structure were plotted through time to examine qualitative patterns of change through community trajectory analysis in the *ecotraj* package (version 0.0.1; De Cáceres et al., 2019). To do this, the 'average' community structure of each treatment group at each timepoint, using abundance and cover data from visual surveys, was determined by averaging species abundance or cover for all experimental tiles in each treatment, and distance-based redundancy analysis was performed on these averaged communities for all timepoints with 999 random starts and autotransformation of data using Bray-Curtis distances.

Differences in the temperature of tile treatments drove divergences in the biological community inhabiting these tiles over time (Fig. A10). Cool and warm treatments quickly diverged in composition over the first summer, and this divergence grew through the winter.

Communities followed a similar trajectory during the first part of the second summer. However, treatment differences were apparent by the end of the summer, with CC and WC treatments grouping together and WW and CW treatments grouping together. Following the second winter, the WW and CC treatments were quite similar in composition to the warm and cool treatments, respectively, at the same time the previous year, while the CW and WC treatments were intermediate in their composition.

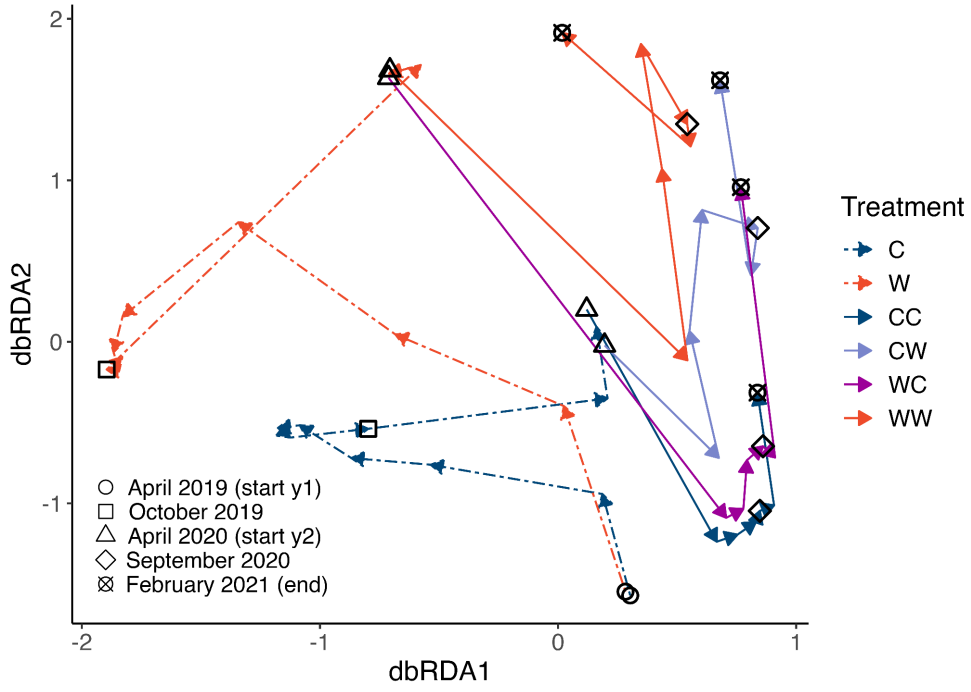

Figure A10. Trajectory plot for experimental tile communities over the course of the experiment from April 2019 to February 2021. Trajectories represent the 'average' community — calculated by averaging the abundance of each species across experimental tile units in each treatment at each timepoint — with the start and end terminus of each arrow based on Bray-Curtis dissimilarities among communities. The direction of arrows shows the flow of time from the beginning to the end of the experiment, and the length of each arrow correlates with the magnitude of community shift between timepoints. Different points along each treatment trajectory help visually identify key timepoints during the experiment (experiment start, end of summer in y1=year one, start of y2=year two, end of summer in y2, experiment end). Sample sizes for each treatment group changes through time. See Fig. A2 for treatment abbreviations.

Epifaunal communities

Table A2. Inventory of epifaunal taxa found during destructive surveys of intertidal barnacle bed communities on experimental tiles at TESNO, EN.

Taxon name	Authority
Amiphopoda	Latreille, 1816
Anthopleura elegantissima	Brandt, 1835
Annelida	
Arachnida	
Cyprid larva	Burmeister, 1834
Copepoda	Milne Edwards, 1840
Dynamenella sheareri	Hatch, 1947
Emplectonema gracile	Johnston, 1837
Hymenoptera	
Insecta	
Isopoda	Latreille, 1817
Lasaea rubra	Montagu, 1803
Littorina scutulata	Gould, 1849
Littorina sitkana	Philippi, 1846
Lottia digitalis	Rathke, 1833
Lottia paradigitalis	Fritchman, 1960
Lottia pelta	Rathke, 1833
Lottia scutum	Rathke, 1833
Lottia sp.	Gray, 1833
Mytilus sp.	Linnaeus, 1758
Neostylidium eschrichtii	Middendorff, 1849
Nemertea	
Oedoparena sp.	Curran, 1934
Onchidoris bilamellata	Linnaeus, 1767
Pagurus hirsutiusculus	Dana, 1851
Platyhelminthes	Minot, 1876
Polychaeta	Grube, 1850
Polychaeta	Grube, 1850
Sabellidae	Latreille, 1825
Syllidae	Grube, 1850

Appendix 2: Statistical outputs of models from 'The effect of single versus successive warm summers on a high intertidal barnacle bed community'

Analysis 1: Substratum temperature

Model A1

Maximum daily temperature ~ treatment + (1|block/number) + (1|date)
Family: Gaussian

Table A3. Model summary table for Model A1, a linear mixed effects model testing the effect of treatment on the maximum daily temperature of experimental tiles in the first year of the passive warming experiment. Coefficients given are relative to the cool treatment, and the model was tested using a Type I ANOVA. SE = standard error, df = degrees freedom.

Term	Coefficient	SE	Sum Sq.	*F*	df (numerator)	df (denominator)	p
Intercept	28.22	0.87					
Treatment–Rock	1.859	0.665	209.6	35.83	2	71.94	**$3.49 \cdot 10^{-6}$**
Treatment–Warm	1.873	0.354					

Table A4. Tukey-Kramer *post hoc* comparison of the maximum daily temperatures within treatment groups in year one of the passive warming experiment. SE = standard error, C = cool treatment, W = warm treatment

Contrast	Estimate	SE	*z* ratio	p
C–Rock	-1.859	0.665	-2.80	**0.0144**
C–W	-1.873	0.354	-5.29	**<0.0001**
Rock–W	-0.014	0.665	-0.021	1.00

Model A2

Maximum daily temperature ~ treatment + (1|block/number) + (1|date)
Family: Gaussian

Table A5. Model summary table for Model A2, a linear mixed effects model testing the effect of ttreatment on the maximum daily temperature of experimental tiles in the second year of the experiment. Coefficients given are relative to the cool summer – cool summer (CC) treatment, and the model was tested using a Type I ANOVA. SE = standard error, df = degrees freedom. CW = cool summer – warm summer, WC = warm summer – warm summer, WW = warm summer – warm summer.

Term	Coefficient	SE	Sum Sq.	*F*	df (numerator)	df (denominator)	p
Intercept	28.35	0.80					
Treatment–CW	2.207	0.459					
Treatment–Rock	0.8339	0.6460	179.6	10.49	4	66.01	**$1.23 \cdot 10^{-6}$**
Treatment–WC	0.0682	0.4423					
Treatment–WW	2.089	0.466					

Table A6. Tukey-Kramer *post hoc* comparison of the maximum daily temperature of treatment groups in year two of the passive warming experiment. See Table A5 for treatment codes and abbreviations.

Contrast	Estimate	SE	*z* ratio	p
CC–CW	-2.207	0.459	-4.81	**<0.0001**
CC–Rock	-0.834	0.646	-1.29	0.697
CC-WC	-0.068	0.442	-0.15	0.999
CC–WW	-2.089	0.466	-4.49	**<0.0001**
CW–Rock	1.373	0.654	2.10	0.221
CW–WC	2.139	0.456	4.69	**<0.0001**
CW–WW	0.118	0.475	0.25	0.999
Rock–WC	0.766	0.645	1.19	0.758
Rock–WW	-1.255	0.659	-1.91	0.315
WC–WW	-2.021	0.463	-4.37	**0.0001**

Model A3

Mean daily temperature ~ treatment + (1|block/number) + (1|date)
Family: Gaussian

Table A7. Model summary table for Model A3, a linear mixed effects model testing the effect of treatment on the mean daily temperature of experimental tiles in the first year of the passive warming experiment. Coefficients given are relative to the cool treatment, and the model was tested using a Type I ANOVA. See Table A5 for abbreviations.

Term	Coefficient	SE	Sum Sq.	*F*	df (numerator)	df (denominator)	p
Intercept	22.15	0.57					
Treatment–Rock	1.873	0.446					
Treatment–Warm	1.089	0.235	79.77	15.58	2	72.84	**$2.32 \cdot 10^{-6}$**

Table A8. Tukey-Kramer *post hoc* comparison of the maximum daily temperature of treatment groups in year one of the passive warming experiment. SE = standard error, C = cool treatment, W = warm treatment

Contrast	Estimate	SE	*z* ratio	p
C–Rock	-1.873	0.443	-4.23	**<0.0001**
C–W	-1.089	0.235	-4.63	**<0.0001**
Rock–W	0.784	0.443	1.77	0.180

Table A9. Model summary table for Model A3, a linear mixed effects model testing the effect of temperature treatment on the mean daily temperature of experimental tiles in the second year of the experiment. Coefficients given are relative to the cool summer – cool summer (CC) treatment, and the model was tested using a Type I ANOVA. See Table A5 for abbreviations.

Term	Coefficient	SE	Sum Sq.	F	df (numerator)	df (denominator)	p
Intercept	22.03	0.56					
Treatment–CW	1.323	0.287					
Treatment–Rock	1.020	0.405					
Treatment–WC	0.1469	0.2769	80.83	10.08	4	66.63	**$1.93 \cdot 10^{-6}$**
Treatment–WW	1.383	0.291					

Table A10. Tukey-Kramer *post hoc* comparison of mean daily temperature of treatment groups in year two of the passive warming experiment. See Table A5 for treatment codes and abbreviations.

Contrast	Estimate	SE	*z* ratio	p
CC–CW	-1.323	0.287	-4.61	**<0.0001**
CC–Rock	-1.020	0.405	-2.52	0.0870
CC-WC	-0.147	0.277	-0.53	0.984
CC–WW	-1.383	0.291	-4.75	**<0.0001**
CW–Rock	0.304	0.411	0.74	0.947
CW–WC	1.176	0.286	4.12	**0.0004**
CW–WW	-0.060	0.298	-0.20	1.00
Rock–WC	0.873	0.405	2.16	0.196
Rock–WW	-0.364	0.413	-0.88	0.905
WC–WW	-1.236	0.289	-4.27	**0.0002**

Model A4

Maximum temperature ~ treatment + (1|block)
Family: Gaussian

Table A11. Model summary table for Model A4, a linear mixed effects model testing the effect of treatment on the maximum temperature of experimental tiles in the first year of the passive warming experiment. Coefficients given are relative to the cool treatment, and the model was tested using a Type I ANOVA. See Table A5 for abbreviations.

Term	Coefficient	SE	Sum Sq.	*F*	df (numerator)	df (denominator)	p
Intercept	38.5	0.4					
Treatment–Rock	-0.3	0.8					
Treatment–Warm	3.1	0.4	194.68	33.46	2	72.62	**5.01×10^{-11}**

Table A12. Tukey-Kramer *post hoc* comparison of the maximum temperature of treatment groups in year one of the passive warming experiment. SE = standard error, C = cool treatment, W = warm treatment

Contrast	Estimate	SE	df	*t* ratio	p
C–Rock	0.27	0.75	72.1	0.36	0.931
C–W	-3.13	0.40	73.3	-7.75	**<0.0001**

Rock–W	-3.40	0.75	72.1	-4.52	**0.0001**	

Table A13. Model summary table for Model A3, a linear mixed effects model testing the effect of treatment on the maximum temperature of experimental tiles in the second year of the experiment. Coefficients given are relative to the cool summer – cool summer (CC) treatment, and the model was tested using a Type I ANOVA. See Table A5 for abbreviations.

Term	Coefficient	SE	Sum Sq.	F	df (numerator)	df (denominator)	p
Intercept	37.5	0.7					
Treatment–CW	3.3	0.7					
Treatment–Rock	-0.02	1.0	178.3	9.36	4	67.15	**4.50×10^{-6}**
Treatment–WC	0.2	0.7					
Treatment–WW	3.0	0.7					

Table A14. Tukey-Kramer *post hoc* comparison of the maximum temperature of treatment groups in year two of the passive warming experiment. See Table A5 for treatment codes and abbreviations.

Contrast	Estimate	SE	df	*t* ratio	p
CC–CW	-3.323	0.735	67.6	-4.52	**0.0002**
CC–Rock	0.016	1.024	67.2	0.016	1.00
CC-WC	-0.154	0.709	67.2	-0.22	1.00
CC–WW	-2.971	0.747	67.7	-3.97	**0.0016**
CW–Rock	3.339	0.411	67.0	3.22	**0.0163**
CW–WC	3.169	0.731	67.2	4.34	**0.0005**
CW–WW	0.352	0.761	67.1	0.46	0.990
Rock–WC	-0.170	1.022	67.0	-0.17	1.00
Rock–WW	-2.987	1.045	67.1	-2.86	**0.0436**
WC–WW	-2.817	0.743	67.3	-3.79	**0.0029**

Model A5

Balanus glandula recruit year 1 abundance ~ $treatment_{y1}$ + (1|block)
Family: Quasi-Poisson

Table A15. Model summary table for Model A5, a generalized linear mixed effects model of *B. glandula* recruit abundance on experimental tiles during peak recruitment in the first year of the passive warming experiment. Coefficients given are relative to the cool treatment, and the model was tested using a Type II ANOVA. See Table A5 for abbreviations; $Treatment_{y1}$ = treatment in year one.

Term	Coefficient	SE	χ^2	df	p
Intercept	5.187	0.319			
$Treatment_{y1}$	-0.0391	0.2292	0.048	1	0.865

Model A6

Balanus glandula recruit year 2 abundance ~ $treatment_{y1}$ * $treatment_{y2}$ + (1|block)
Family: Quasi-Poisson

Table A16. Model summary table for Model A6, a generalized linear mixed effects model of *B. glandula* recruit abundance on experimental tiles during peak recruitment in the first year of the passive warming experiment. Coefficients given are relative to the cool treatment, and the model was tested using a Type III ANOVA. See Table A5 for abbreviations; $treatment_{y1}$ = treatment in year one, $treatment_{y2}$ = treatment in year two.

Term	Coefficient	SE	χ^2	df	p
Intercept	4.934	0.159			
$Treatment_{y1}$	-0.3884	0.1576	6.07	1	**0.0138**
$Treatment_{y2}$	-1.301	0.210	38.34	1	**5.94×10^{-10}**
$Treatment_{y1}$ * $Treatment_{y2}$	0.3537	0.2900	1.49	1	0.223

Table A17. Tukey-Kramer *post hoc* comparison of *B. glandula* recruitment between treatment groups in year two of the passive warming experiment. See Table A5 for treatment codes and abbreviations.

Contrast	Estimate	SE	df	*z* ratio	p
CC–WC	0.388	0.158	Inf	2.46	0.0657
CC–CW	1.301	0.210	Inf	6.19	**<0.0001**
CC–WW	1.335	0.193	Inf	6.91	**<0.0001**
WC–CW	0.912	0.220	Inf	4.15	**0.0002**
WC–WW	0.947	0.206	Inf	4.60	**<0.0001**
CW–WW	0.035	0.242	Inf	0.14	0.999

Model A7

Chthamalus dalli recruit year 1 abundance ~ treatment_{y1} + (1|block)
Family: Quasi-Poisson

Table A18. Model summary table for Model A7, a generalized linear mixed effects model of *B. glandula* recruit abundance on experimental tiles during peak recruitment in the first year of the passive warming experiment. Coefficients given are relative to the cool treatment, and the model was tested using a Type II ANOVA. See Table A5 and A16 for abbreviations.

Term	Coefficient	SE	χ^2	df	p
Intercept	2.570	0.429			
Treatment_{y1}	-0.6916	0.6057	1.30	1	0.254

Model A8

Chthamalus dalli recruit year 2 abundance ~ $treatment_{y1}$ * $treatment_{y2}$ + (1|block)
Family: Quasi-Poisson

Table A19. Model summary table for Model A8, a generalized linear mixed effects model of *B. glandula* recruit abundance on experimental tiles during peak recruitment in the first year of the passive warming experiment. Coefficients given are relative to the cool treatment, and the model was tested using a Type III ANOVA. See Table A5 and A16 for abbreviations.

Term	Coefficient	SE	χ^2	df	p
Intercept	3.347	0.208			
$Treatment_{y1}$	-0.392	0.166	5.56	1	**0.0184**
$Treatment_{y2}$	-0.852	0.195	19.16	1	**1.20×10^{-5}**
$Treatment_{y1}$ * $Treatment_{y2}$	0.430	0.272	2.50	1	0.114

Table A20. Tukey-Kramer *post hoc* comparison of *C. dalli* recruitment between treatment groups in year two of the passive warming experiment. See Table A5 for treatment codes and abbreviations.

Contrast	Estimate	SE	df	*z* ratio	p
CC–WC	0.392	0.158	Inf	2.36	0.0856
CC–CW	0.852	0.195	Inf	4.38	**0.0001**
CC–WW	0.815	0.178	Inf	4.58	**<0.0001**
WC–CW	0.460	0.208	Inf	2.22	0.119
WC–WW	0.423	0.192	Inf	2.20	0.124
CW–WW	-0.038	0.215	Inf	-0.18	0.998

Model A9

Balanus glandula year 1 adult abundance ~ treatment_{y1} + (1|block)
Family: Quasi-Poisson

Table A21. Model summary table for Model A9, a generalized linear mixed effects model of adult *B. glandula* abundance on experimental tiles at the end of the first year of the passive warming experiment. Coefficients given are relative to the cool treatment, and the model was tested using a Type II ANOVA. See Table A5 and A16 for abbreviations

Term	Coefficient	SE	χ^2	df	p
Intercept	3.237	0.275			
Treatment_{y1}	-1.524	0.148	106.20	1	**$<2.2\text{x}10^{-16}$**

Model A10

Balanus glandula year 2 adult abundance ~ treatment_{y1} * treatment_{y2} + (1|block)
Family: Quasi-Poisson

Table A22. Model summary table for Model A10, a generalized linear mixed effects model of adult *B. glandula* abundance on experimental tiles at the end of the second year of the passive warming experiment. Coefficients given are relative to the cool treatment, and the model was tested using a Type III ANOVA. See Table A5 and Table A16 for abbreviations.

Term	Coefficient	SE	χ^2	df	p
Intercept	3.487	0.379			
Treatment_{y1}	-0.822	0.477	2.97	1	0.0846
Treatment_{y2}	-0.807	0.505	2.55	1	0.110
Treatment_{y1} * Treatment_{y2}	0.156	0.715	0.048	1	0.827

Table A23. Tukey-Kramer *post hoc* comparison of adult *B. glandula* abundance between treatment groups in year two of the passive warming experiment. See Table A5 for treatment codes and abbreviations.

Contrast	Estimate	SE	df	*z* ratio	p
CC–WC	0.822	0.477	Inf	1.73	0.311
CC–CW	0.807	0.505	Inf	1.60	0.380
CC–WW	1.473	0.478	Inf	3.08	**0.0111**
WC–CW	-0.016	0.551	Inf	-0.028	1.00
WC–WW	0.651	0.525	Inf	1.24	0.601
CW–WW	0.666	0.535	Inf	1.25	0.598

Model A11

Chthamalus dalli year 1 adult abundance ~ treatment_{y1} + (1|block)
Family: Quasi-Poisson

Table A24. Model summary table for Model A11, a generalized linear mixed effects model of adult *C. dalli* abundance on experimental tiles at the end of the first year of the passive warming experiment. Coefficients given are relative to the cool treatment, and the model was tested using a Type II ANOVA. See Table A5 and Table A16 for abbreviations.

Term	Coefficient	SE	χ^2	df	p
Intercept	-1.654	0.572			
Treatment_{y1}	-0.287	0.356	0.65	1	0.420

Model A12

Chthamalus dalli year 2 adult abundance ~ $treatment_{y1}$ * $treatment_{y2}$ + (1|block)
Family: Quasi-Poisson

Table A25. Model summary table for Model A12, a generalized linear mixed effects model of adult *C. dalli* abundance on experimental tiles at the end of the second year of the passive warming experiment. Coefficients given are relative to the cool treatment, and the model was tested using a Type III ANOVA. See Table A5 and Table A16 for abbreviations.

Term	Coefficient	SE	χ^2	df	p
Intercept	3.080	0.408			
$Treatment_{y1}$	-0.502	0.462	1.18	1	0.277
$Treatment_{y2}$	-0.239	0.490	0.24	1	0.626
$Treatment_{y1}$ * $Treatment_{y2}$	-0.139	0.685	0.041	1	0.840

Table A26. Tukey-Kramer *post hoc* comparison of adult *C. dalli* abundance between treatment groups in year two of the passive warming experiment. See Table A5 for treatment codes and abbreviations.

Contrast	Estimate	SE	df	*z* ratio	p
CC–WC	0.502	0.462	Inf	1.09	0.698
CC–CW	0.239	0.490	Inf	0.49	0.962
CC–WW	0.879	0.450	Inf	1.95	0.207
WC–CW	-0.263	0.518	Inf	-0.51	0.957
WC–WW	0.377	0.487	Inf	0.77	0.866
CW–WW	0.641	0.500	Inf	1.28	0.575

Model A13

Lottia spp. abundance ~ treatment_{y1} * treatment_{y2} + date + (1|block)
Family: Quasi-Poisson

Table A27. Model summary table for Model A13, a generalized linear mixed effects model of *Lottia* spp. abundance on experimental tiles. Data were collected at the end of the second summer and in late winter, on 14 September 2020 and 21 February 2021. Coefficients for treatment are given are relative to the cool treatment, and the model was tested using a Type III ANOVA. See Table A5 and Table A16 for abbreviations.

Term	Coefficient	SE	χ^2	df	p
Intercept	0.758	0.507			
Treatment_{y1}	-0.413	0.204	4.10	1	**0.0428**
Treatment_{y2}	-0.747	0.268	7.75	1	**0.00537**
Date	0.794	0.181	19.21	1	**1.17×10^{-5}**
Treatment_{y1} * Treatment_{y2}	-0.348	0.409	0.72	1	0.395

Table A28. Tukey-Kramer *post hoc* comparison of *Lottia* spp. abundance between treatment groups in year two of the passive warming experiment. See Table A5 for treatment codes and abbreviations.

Contrast	Estimate	SE	df	*z* ratio	p
CC–WC	0.413	0.204	Inf	2.03	0.179
CC–CW	0.747	0.268	Inf	2.78	**0.0275**
CC–WW	1.507	0.301	Inf	5.02	**<0.0001**
WC–CW	0.334	0.285	Inf	1.17	0.644
WC–WW	1.094	0.314	Inf	3.48	**0.00280**
CW–WW	0.760	0.355	Inf	2.14	0.140

Model A24

Littorina spp. abundance ~ $treatment_{y1}$ * $treatment_{y2}$ + date + (1|block)
Family: Quasi-Poisson

Table A29. Model summary table for Model A14, a generalized linear mixed effects model of *Littorina* spp. abundance on experimental tiles. Data were collected at the end of the second summer and in late winter, on 14 September 2020 and 21 February 2021. Coefficients given are relative to the cool treatment, and the model was tested using a Type III ANOVA. See Table A5 and Table A16 for abbreviations.

Term	Coefficient	SE	χ^2	df	p
Intercept	4.096	0.200			
$Treatment_{y1}$	-1.044	0.219	22.82	1	**1.78×10^{-6}**
$Treatment_{y2}$	-0.976	0.224	18.97	1	**1.33×10^{-5}**
Date	-1.608	0.228	49.65	1	**1.84×10^{-12}**
$Treatment_{y1}$ * $Treatment_{y2}$	0.377	0.343	1.21	1	0.272

Table A30. Tukey-Kramer *post hoc* comparison of *Littorina* spp. abundance between treatment groups in year two of the passive warming experiment. See Table A5 for treatment codes and abbreviations.

Contrast	Estimate	SE	df	*z* ratio	p
CC–WC	1.044	0.219	Inf	4.78	**<0.0001**
CC–CW	0.976	0.224	Inf	4.36	**0.0001**
CC–WW	1.644	0.238	Inf	6.91	**<0.0001**
WC–CW	-0.068	0.253	Inf	-0.28	0.993
WC–WW	0.600	0.261	Inf	2.30	0.0982
CW–WW	0.667	0.269	Inf	2.48	0.0624

Model A15

Algal cover ~ treatment + s(time) + s(time, by = treatment) + s(block, type = "re")

Family: Gaussian

Table A31. Model summary table for Model A15, a generalized additive mixed model of differences in algal cover over time between treatments in the first year of the experiment. Estimates and differences between smooth functions are given relative to the cool treatment. See table A5 for abbreviations.

Component	Term	Estimate	SE	t	p
Parametric	Intercept	32.613	1.989	16.40	**$<2x10^{-16}$**
	Treatment: W	-1.097	1.380	-0.80	0.427
		Effective df		**F**	**p**
Smooth	s(time)	7.47		98.97	**$<2x10^{-16}$**
	s(time):W	5.90		12.61	**$<2x10^{-16}$**
	s(block)	4.30		6.41	**$1.45x10^{-6}$**

Table A31. Model summary table for Model A15, a generalized additive mixed model of differences in algal cover over time between treatments in the second year of the experiment. Estimates and differences between smooth functions are given relative to the cool treatment. k=5 for smoothing functions of time. See table A5 for abbreviations.

Component	Term	Estimate	SE	t	p
Parametric	Intercept	2.562	1.175	2.18	**0.0297**
	Treatment: CW	2.661	1.454	1.83	0.0678
	Treatment: WC	1.907	1.404	1.36	0.175
	Treatment: WW	0.120	1.330	0.091	0.928
		Effective df		**F**	**p**
Smooth	s(time)	3.92		20.83	**$<2x10^{-16}$**
	s(time):CW	2.36		2.87	0.108
	s(time):WC	1.82		7.47	**0.00593**
	s(time):WW	1.00		1.20	0.275
	s(block)	3.19		1.81	**0.0152**

Model A16

Species richness ~ $treatment_{y1}$ * date + (1|block)
Family: Poisson

Table A32. Model summary table for Model A18, a generalized linear mixed effects model of the species richness on experimental tile communities during the first year. Data were collected at the end of the summer, on 20 October 2019, and during the winter, on 15 March 2020. Coefficients given are relative to the cool treatment, and the model was tested using a Type III ANOVA. See Table A5 and Table A16 for abbreviations.

Term	Coefficient	SE	χ^2	df	p
Intercept	1.342	0.140			
$Treatment_{y1}$	-0.457	0.115	15.52	1	**8.15×10^{-5}**
Date	-0.163	0.095	2.98	1	0.0845
$Treatment_{y1}$ * Date	-0.503	0.160	9.85	1	**0.00170**

Model A17

Species richness ~ $treatment_{y1}$ * $treatment_{y2}$ + date + (1|block)
Family: Poisson

Table A33. Model summary table for Model A19, a generalized linear mixed effects model of the species richness of experimental tiles during the second year. Data were collected at the end of the summer, on 14 September 2020, and during winter, on 24 February 2021. Coefficients given are relative to the cool treatment, and the model was tested using a Type III ANOVA. See Table A5 and Table A16 for abbreviations.

Term	Coefficient	SE	χ^2	df	p
Intercept	1.696	0.097			
$Treatment_{y1}$	-0.093	0.112	0.70	1	0.403
$Treatment_{y2}$	-0.221	0.123	3.25	1	0.0714
Date	-0.115	0.090	1.62	1	0.203
$Treatment_{y1}$ * $Treatment_{y2}$	-0.173	0.172	1.01	1	0.314

Table A34. Tukey-Kramer *post hoc* comparison of species richness between treatment groups in year two of the passive warming experiment. See Table A5 for treatment codes and abbreviations.

Contrast	Estimate	SE	df	*z* ratio	p
CC–WC	0.093	0.112	Inf	0.84	0.838
CC–CW	0.221	0.123	Inf	1.80	0.272
CC–WW	0.487	0.117	Inf	4.15	**2.00×10^{-4}**
WC–CW	0.128	0.121	Inf	1.01	0.742
WC–WW	0.394	0.121	Inf	3.26	**0.00620**
CW–WW	0.266	0.130	Inf	2.04	0.174

Model A20

Invertebrate Shannon diversity ~ treatment_{y1} + date + (1|block)
Family: Tweedie
Dispersion formula: ~ treatment_{y1}

Table A35. Model summary table for Model A20, a generalized linear mixed effects model of the invertebrate Shannon diversity of experimental tile communities during the first year. Data were collected at the end of the summer, on 20 October 2019, and during winter, on 15 March 2020. Coefficients given are relative to the cool treatment, and the model was tested using a Type III ANOVA. See Table A5 and Table A9 for abbreviations.

Term	Coefficient	SE	χ^2	df	p
Intercept	-1.122	0.229			
Treatment_{y1}	-0.071	0.232	0.092	1	0.761
Date	-0.009	0.142	0.0039	1	0.950
Treatment_{y1} * Date	-1.343	0.372	13.01	1	**3.09×10^{-4}**
Dispersion model					
Intercept	-1.435	0.089			
Treatment_{y1}	1.131	0.095			

Model A21

Invertebrate Shannon diversity ~ $treatment_{y1}$ * $treatment_{y2}$ + date + (1|block)
Family: Tweedie

Table A36. Model summary table for Model A21, a generalized linear mixed effects model of the invertebrate Shannon diversity of experimental tiles during the second year. Data were collected at the end of the summer, on 14 September 2020, and during the winter, on 24 February 2021 . Coefficients given are relative to the cool treatment, and the model was tested using a Type III ANOVA. See Table A5 and Table A9 for abbreviations.

Term	Coefficient	SE	χ^2	df	p
Intercept	1.254	0.070			
$Treatment_{y1}$	-0.246	0.080	9.37	1	**0.00220**
$Treatment_{y2}$	-0.163	0.085	3.69	1	0.0546
Date	-0.381	0.059	41.80	1	**1.01×10^{-10}**
$Treatment_{y1}$ * $Treatment_{y2}$	-0.017	0.114	0.022	1	0.883

Table A37. Tukey-Kramer *post hoc* comparison of invertebrate Shannon diversity between treatment groups in year two of the passive warming experiment. See Table A5 for treatment codes and abbreviations.

Contrast	Estimate	SE	df	*t* ratio	p
CC–WC	0.246	0.080	124	3.06	**0.0142**
CC–CW	0.163	0.085	124	1.92	0.224
CC–WW	0.425	0.076	124	5.60	**<0.0001**
WC–CW	-0.083	0.086	124	-0.97	0.766
WC–WW	0.179	0.077	124	2.33	0.0962
CW–WW	0.263	0.081	124	3.24	**0.0084**

Model A22

Algal Shannon diversity ~ $treatment_{y1}$ + date + (1|block)
Family: Tweedie

Table A38. Model summary table for Model A22, a generalized linear mixed effects model of the algal Shannon diversity of experimental tile communities. Data were collected at the end of the first summer following exposure to heat stress, on 20 October 2019. Coefficients given are relative to the cool treatment, and the model was tested using a Type II ANOVA. See Table A5 and Table A9 for abbreviations.

Term	Coefficient	SE	χ^2	df	p
Intercept	-2.444	0.490			
$Treatment_{y1}$	-1.341	0.358	14.01	1	**1.82×10^{-4}**
Date	-0.014	0.329	0.0018	1	0.966

Model A23

Algal Shannon diversity ~ $treatment_{y1}$ * $treatment_{y2}$ + (1|block)
Family: Tweedie

Table A39. Model summary table for Model A23, a generalized linear mixed effects model of the algal Shannon diversity of experimental tiles. Data were collected at the end of the first winter following recovery from heat stress, on 24 February 2021. Coefficients given are relative to the cool treatment, and the model was tested using a Type III ANOVA. See Table A5 and Table A9 for abbreviations.

Term	Coefficient	SE	χ^2	df	p
Intercept	-1.609	0.507			
$Treatment_{y1}$	0.7698	0.6407	1.444	1	0.230
$Treatment_{y2}$	-0.3348	0.8722	0.147	1	0.701
$Treatment_{y1}$ * $Treatment_{y2}$	-1.105	1.114	0.984	1	0.321

Table A40. Tukey-Kramer *post hoc* comparison of algal Shannon diversity between treatment groups in year two of the passive warming experiment. See Table A5 for treatment codes and abbreviations.

Contrast	Estimate	SE	df	z ratio	p
CC–WC	-0.770	0.641	Inf	-1.20	0.626
CC–CW	0.335	0.872	Inf	0.38	0.981
CC–WW	0.670	0.765	Inf	0.88	0.818
WC–CW	1.105	0.810	Inf	1.35	0.522
WC–WW	1.440	0.693	Inf	2.08	0.161
CW–WW	0.335	0.912	Inf	0.37	0.983

Model A24

Species assemblage ~ treatment

Table A41. Model summary table of PERMANOVA output for Model A24 describing differences in epifaunal community composition of experimental tiles destructively sampled on 14 September 2020. PERMANOVA uses constrained ordination via distance-based redundancy analyses with Bray-Curtis distances. df = degrees of freedom.

Term	df	Sum of squares	F	p
Treatment	3	1.145	1.495	0.0566
Residuals	31	7.913		

Table A42. Multiple pairwise comparisons of epifaunal community composition across treatments using constrained ordination via distance-based redundancy analyses with Bray-Curtis distances. Epifauna were destructively sampled on 14 September 2020. df = degrees of freedom

Comparison	df	Sum of squares	F	p
CC – CW	1	0.2726	1.164	0.277
CC – WC	1	0.2760	1.213	0.292
CC – WW	1	0.7796	2.705	**0.028**
CW – WC	1	0.04749	0.2157	0.985
CW – WW	1	0.4542	1.595	0.136
WC – WW	1	0.4386	1.595	0.134

Table A43. Model summary table of PERMANOVA output for Model A24 describing differences in epifaunal community composition of experimental tiles destructively sampled on 24 February 2021. PERMANOVA uses constrained ordination via distance-based redundancy analyses with Bray-Curtis distances. df = degrees of freedom.

Term	df	Sum of squares	F	p
Treatment	3	2.589	3.341	**0.0001**
Residuals	37	9.558		

Table A44. Multiple pairwise comparisons of epifaunal community composition across treatments using constrained ordination via distance-based redundancy analyses with Bray-Curtis distances. Epifauna were destructively sampled on 24 February 2021. df = degrees of freedom

Comparison	df	Sum of squares	F	p
CC – CW	1	0.9604	4.189	**0.009**
CC – WC	1	0.6442	2.448	**0.024**
CC – WW	1	1.757	6.833	**0.002**
CW – WC	1	0.1765	0.6794	0.702
CW – WW	1	0.4500	1.781	0.112
WC – WW	1	0.9809	3.497	**0.005**

Model A25

Species assemblage heterogeneity ~ treatment

Table A45. Model summary table of PERMDISP output for Model A25 of differences in epifaunal community composition heterogeneity of experimental tiles destructively sampled in September 2020. df = degrees of freedom.

Term	df	Sum of squares	Mean squares	F	p
Treatment	3	0.07327	0.02442	2.616	0.0686
Residuals	31	0.2894	0.0093		

Table A46. Model summary table of PERMDISP output for Model A25 of differences in epifaunal community composition heterogeneity of experimental tiles destructively sampled in February 2021. df = degrees of freedom.

Variable	df	Sum of squares	Mean squares	F	p
Treatment	3	0.03230	0.01077	0.5967	0.621
Residuals	37	0.6676	0.0180		

Model A26

Species richness ~ $treatment_{y1}$ * $treatment_{y2}$ + date
Family: Poisson

Table A47. Model summary table for Model A26, a generalized linear mixed effects model of the species richness of epifauna from destructively sampled tile communities collected on 14 September 2020 and 24 February 2021. Coefficients given are relative to the cool treatment, and the model was tested using a Type III ANOVA. See Table A5 and Table A9 for abbreviations.

Term	Coefficient	SE	χ^2	df	p
Intercept	2.303	0.099			
$Treatment_{y1}$	-0.2061	0.1042	3.910	1	**0.0480**
$Treatment_{y2}$	-0.2831	0.1187	5.686	1	**0.0171**
Date	0.0185	0.0834	0.0490	1	0.825
$Treatment_{y1}$ * $Treatment_{y2}$	-0.1233	0.1696	0.5283	1	0.467

Table A48. Tukey-Kramer *post hoc* comparison of species richness of epifauna from destructively sampled tile communities between treatment groups in year two of the passive warming experiment. See Table A5 for treatment codes and abbreviations.

Contrast	Estimate	SE	df	z ratio	p
CC–WC	0.206	0.104	Inf	1.98	0.197
CC–CW	0.283	0.119	Inf	2.39	**0.0800**
CC–WW	0.613	0.117	Inf	5.21	**<0.0001**
WC–CW	0.0771	0.123	Inf	0.628	0.923
WC–WW	0.406	0.122	Inf	3.33	**0.00480**
CW–WW	0.329	0.133	Inf	2.47	0.0645

Model A27
Shannon diversity ~ $treatment_{y1}$ * $treatment_{y2}$ + date
Family: Poisson

Table A49. Model summary table for Model A27, a generalized linear mixed effects model of the Shannon diversity of epifauna from destructively sampled tile communities collected on 14 September 2020 and 24 February 2021. Coefficients given are relative to the cool treatment, and the model was tested using a Type III ANOVA. See Table A5 and Table A9 for abbreviations.

Term	Coefficient	SE	χ^2	df	p
Intercept	1.404	0.148			
$Treatment_{y1}$	-0.2478	0.1441	2.957	1	0.0855
$Treatment_{y2}$	-0.2676	0.1578	2.880	1	0.0897
Date	0.0105	0.1074	0.0095	1	0.922
$Treatment_{y1}$ * $Treatment_{y2}$	-0.2753	0.2127	1.676	1	0.195

Table A50. Tukey-Kramer *post hoc* comparison of the Shannon diversity of epifauna from destructively sampled tile communities between treatment groups in year two of the passive warming experiment. See Table A5 for treatment codes and abbreviations.

Contrast	Estimate	SE	df	z ratio	p
CC–WC	0.248	0.144	69	1.72	0.322
CC–CW	0.268	0.158	69	1.70	0.333
CC–WW	0.791	0.144	69	5.51	**<0.0001**
WC–CW	0.020	0.157	69	0.13	0.999
WC–WW	0.543	0.143	69	3.79	**0.0018**
CW–WW	0.523	0.156	69	3.36	**0.0068**